

Synthesis and Characterization of Electron Deficient Asymmetrically Substituted Diarylindenotetracenes

Lafe J. Purvis, Xingxian Gu, Soumen Ghosh, Zhuoran Zhang, Christopher J. Cramer, and Christopher J. Douglas

J. Org. Chem., **Just Accepted Manuscript** • DOI: 10.1021/acs.joc.7b02756 • Publication Date (Web): 23 Jan 2018

Downloaded from <http://pubs.acs.org> on January 23, 2018

Just Accepted

“Just Accepted” manuscripts have been peer-reviewed and accepted for publication. They are posted online prior to technical editing, formatting for publication and author proofing. The American Chemical Society provides “Just Accepted” as a free service to the research community to expedite the dissemination of scientific material as soon as possible after acceptance. “Just Accepted” manuscripts appear in full in PDF format accompanied by an HTML abstract. “Just Accepted” manuscripts have been fully peer reviewed, but should not be considered the official version of record. They are accessible to all readers and citable by the Digital Object Identifier (DOI®). “Just Accepted” is an optional service offered to authors. Therefore, the “Just Accepted” Web site may not include all articles that will be published in the journal. After a manuscript is technically edited and formatted, it will be removed from the “Just Accepted” Web site and published as an ASAP article. Note that technical editing may introduce minor changes to the manuscript text and/or graphics which could affect content, and all legal disclaimers and ethical guidelines that apply to the journal pertain. ACS cannot be held responsible for errors or consequences arising from the use of information contained in these “Just Accepted” manuscripts.

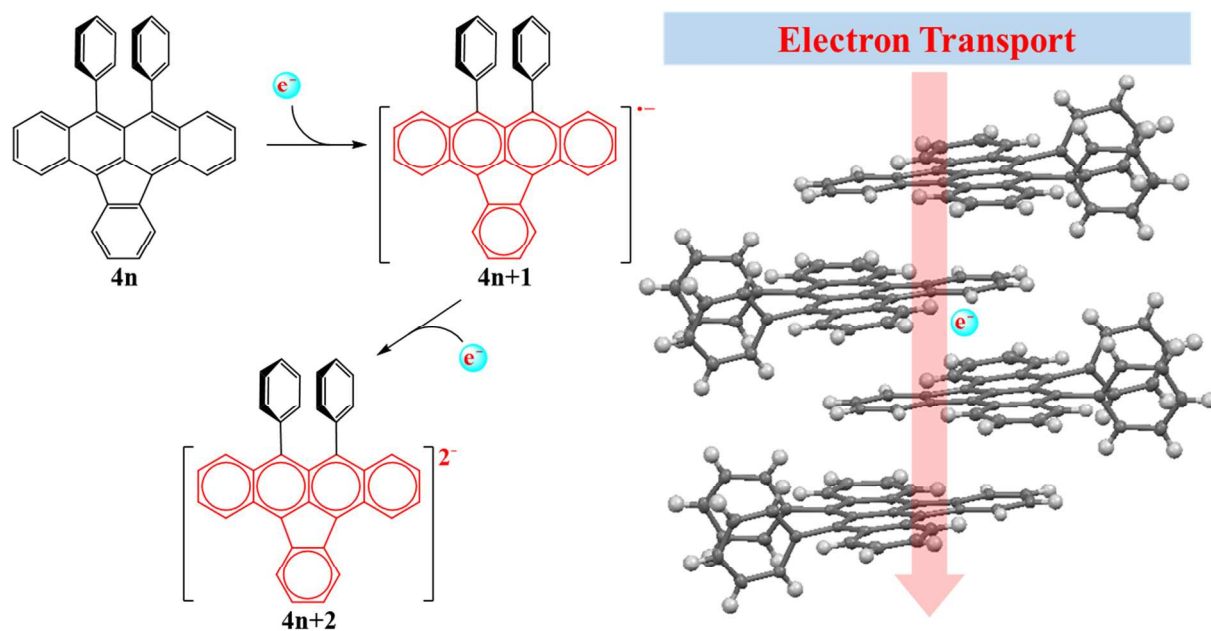


Synthesis and Characterization of Electron Deficient Asymmetrically Substituted Diarylindenotetracenes

Lafe J. Purvis, Xingxian Gu†, Soumen Ghosh, Zhuoran Zhang, Christopher J. Cramer*, and Christopher J. Douglas*

Department of Chemistry, Chemical Theory Center, and Supercomputing Institute, University of Minnesota, Minneapolis, MN, 55455

Graphical abstract



Abstract

Electron deficient asymmetrically substituted diarylindenotetracenes were prepared via a series of Friedel-Crafts acylation's, aryl-aryl cross-couplings, and an intramolecular oxidative

1
2
3 cyclization to form the indene ring. Single crystal X-ray experiments showed good π - π overlap
4 with π - π distances ranging from 3.26 to 3.76 Å. Both thermogravimetric analysis and differential
5 scanning calorimetry indicated that ASIs are stable at elevated temperatures. From Cyclic
6
7
8
9
10 voltammetry experiments HOMO/LUMO energy levels of ASI derivatives were determined to
11 be near -5.4/-4.0 eV. UV/ visible absorption spectra showed strong absorption of light between
12
13
14 400-650 nm with molar attenuation coefficients from 10^4 to 10^5 M⁻¹cm⁻¹. ASI were also found
15
16
17 to have very low fluorescence quantum yields, less than 4%. Using the solid-state packing
18
19
20 determined from the single crystal X-ray experiments, computational modeling indicated that
21
22
23 ASI molecules should favor electron transport.

24 **Introduction**

25
26 Over the past decades the demand for cheaper, faster, and smaller electronic devices has
27
28 driven chemists to discover a large number of new small-molecule, electron-donor, p-type
29
30 materials. Over the same period, however, there has been significantly less development of novel
31
32 small-molecule, electron-acceptor, n-type materials, especially for use in organic solar cells.¹ To
33
34 date, the benchmark electron acceptor material for organic photovoltaics has been the fullerene
35
36 C₆₀, owing to its high electron affinity and efficient, isotropic charge transport.
37
38

39
40 However, despite having good solid-state properties that allow for efficient electron
41
42 transport, fullerenes are not ideal materials for OPVs. The several drawbacks of fullerenes
43
44 include poor solubility in organic solvents, limited stability, and relatively high cost. Another
45
46 drawback of fullerenes is their poor absorption of light in the visible region. In OPVs, this
47
48 relative transparency necessitates a thick absorber layer in order to produce sufficient light-
49
50 generated charge carriers (excitons). Although the thicker absorber layer does result in greater
51
52
53
54
55
56
57
58
59
60

1
2
3 exciton generation, it also decreases charge separation efficiency of the device due to the short
4
5 diffusion length of excitons in the organic material.²⁻⁵
6

7
8 Recently, efforts to overcome the inherent deficiencies of fullerenes led to the
9
10 development of several novel, non-fullerene electron acceptors.⁶⁻¹³ Non-fullerene electron
11
12 acceptors have the potential to greatly improve OPV performance through design of materials
13
14 with strong light absorption, tuned highest occupied molecular orbital (HOMO)/lowest
15
16 unoccupied molecular orbital (LUMO) levels, and improved processability and photostability.¹⁴⁻
17
18 ¹⁶ Among these novel electron acceptors, indene-fused aromatic compounds have shown promise
19
20 as possible replacements for fullerenes in OPVs.¹⁷⁻¹⁹
21
22

23
24 The intrinsic electron deficiency of indene-containing molecules originates from electron
25
26 accepting ability of the conjugated five membered ring. The drive towards aromaticity ($4n+2$)
27
28 makes materials containing indenenes good electron acceptors. The Plunkett group and Haley
29
30 group have independently developed new organic n-type materials based on the indene scaffold
31
32 for use in OPVs.^{8,20,21} Corannulenes may also replace fullerenes as the electron transport layer.²²
33
34 The cyclopentane-fused polycyclic aromatic hydrocarbons and indacene materials demonstrate
35
36 LUMOs below -3.5 eV and HOMOs below -5.5 eV, allowing for n-type behavior. These
37
38 materials also have good solubility in organic solvents and can be readily derivatized.
39
40
41

42
43 Extending the range of indene-based materials as new n-type acceptors, we have prepared
44
45 and studied diarylindenotetracenes. Previously, our group reported on the development of
46
47 symmetrically substituted indenotetracenes.²³ In this article, we report a divergent synthetic
48
49 strategy allowing for rapid diversification and structure–function relationship studies of the
50
51 indenotetracene core. Our new synthetic strategy enabled us to prepare several asymmetrically
52
53 substituted indenotetracene (ASI) derivatives. Beyond the syntheses, we have examined and
54
55
56
57
58
59
60

1
2
3 modeled their electronic and physical properties to evaluate their potential for use as n-type
4 materials in organic photovoltaics.²⁴
5
6

7 RESULTS AND DISCUSSION

10 Synthesis

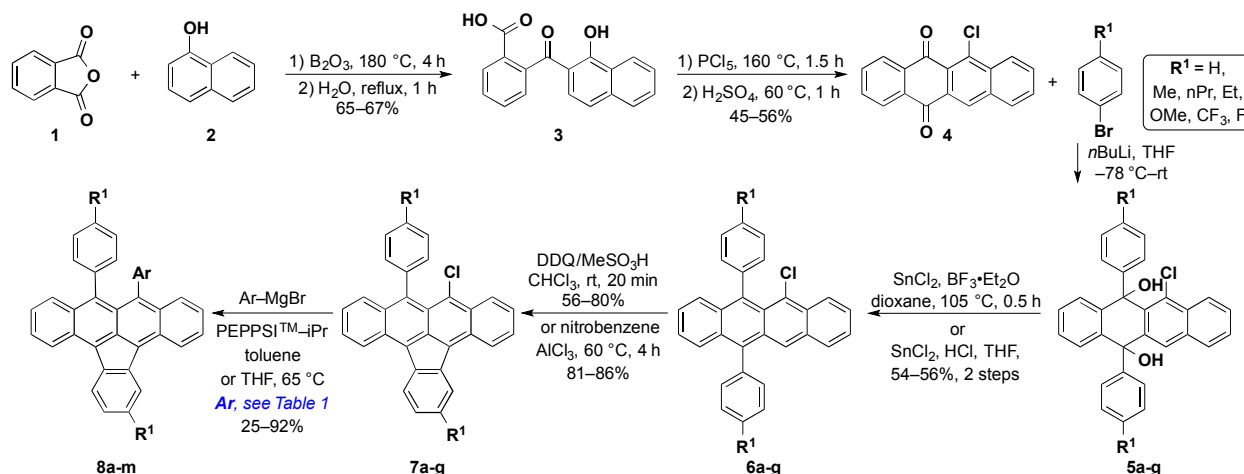
11
12 We began by designing the synthesis of ASIs to allow for late-stage diversification and
13 easy derivatization. This was accomplished via a series of Friedel–Crafts acylations, aryl-aryl
14 cross-coupling reactions, and a Scholl oxidative cyclization (Scheme 1).
15
16
17

18
19 Starting with commercially available phthalic anhydride (**1**) and 1-hydroxyl naphthalene
20 (**2**), 2-(1-hydroxy-2-naphthoyl)benzoic acid, compound (**3**), was obtained via a Friedel–Crafts
21 acylation using the Lewis acid boron trioxide. Following treatment of compound (**3**) with PCl₅
22 and heating in sulfuric acid 6-chlorotetracene-5,12-dione, compound (**4**), was obtained in good
23 yields, 50% over 2 steps.⁹ Using the above conditions compound (**4**) was synthesized on 0.1 M
24 scale, which, was then be used in all subsequent synthesis. The first point of diversification was
25 achieved by treating naphthacenequinone **4** with substituted aryllithium reagents, producing the
26 diol intermediates **5a–g** as mixtures of *syn/anti* isomers. Upon reductive aromatization,
27 compounds **6a–g** became a bright orange/red color indicating that the tetracene core had been
28 successfully formed.^{25,26}
29
30
31
32
33
34
35
36
37
38
39
40
41

42 In the key step of our synthesis we envisioned forming the indene ring via an oxidative
43 cyclization using Scholl reaction conditions.^{27,28} In previous syntheses of rubicene, and other
44 indene containing polycyclic aromatic hydrocarbons (PAH), the indene moieties were prepared
45 via intramolecular palladium-catalyzed aryl-aryl cross-coupling or pentannulation.^{29,30} Scholl
46 reaction conditions have been used in the synthesis of several PAH compounds, and recently,
47 Chi and coworkers synthesized bisindeno-annulated pentacene molecules under Scholl reaction
48
49
50
51
52
53
54
55
56
57
58
59
60

1
2
3 conditions using FeCl₃ as the oxidizing agent.^{31,32} Using two different Scholl reaction conditions,
4
5 compounds **7a–b** were formed via oxidative cyclization using AlCl₃ in nitrobenzene while
6
7
8 compounds **7c–g** were obtained from a solution of chloroform and methanesulfonic acid in the
9
10 presence of 2,3-dichloro-5,6-dicyano-1,4-benzoquinone (DDQ), with yields ranging from 40 to
11
12 86%.^{33,34} The formation of compounds **7a–g** resulted in another color change, from the
13
14 orange/red color of compounds **6a–g**, to a purple/black color. Interestingly, the regiochemistry of
15
16 compounds **7a–g** was found to be very specific. Oxidative cyclization was only observed to occur
17
18 at the C12 of the tetracene core and never at the C10. We attributed this high region-selectivity to
19
20 steric-repulsion between the C5 chloride and the C6 phenyl group. This steric-repulsion pushes
21
22 carbons 5 and 6 away from each other, which, in turn pushes the C11 phenyl group closer to the
23
24 C12 hydrogen.
25
26
27

28
29 From compounds **7a–g**, we performed the final late-stage diversification using Kumada-
30
31 Corriu cross-coupling conditions previously developed in our lab to produce compounds **8a–m**
32
33 in yields between 40 and 92%.^{23,35,36} We found that, in most cases, the primary impurities in the
34
35 crude reaction mixtures were the unreacted starting material and dehalogenated compound (**7**).
36
37 These impurities were readily separable from the desired product by either column
38
39 chromatography and/or recrystallization, the only exception being compound **8d**.³⁷ We were
40
41 unable to find purification conditions which separated unreacted starting material **7d** from
42
43 product **8d**. In order to obtain pure **8d** the reaction had to be driven to completion then
44
45 recrystallization could be performed to remove any additional impurities.
46
47
48
49
50
51
52
53
54
55
56
57
58
59
60



Scheme 1: Synthesis of asymmetric indenotetracenes **8a-m**

Table 1: Functional groups at R¹ and Ar and the yield of three key steps, preparation of **6-8**.

Entry	R ¹	6 , % yield	7 , % yield	Ar	8 , % yield
1	H	6a , 80 ^a	7a , 81	Ph ^c	8a , 60
2	H			<i>p</i> -C ₆ H ₄ F ^c	8h , 51
3	H			<i>p</i> -tol ^c	8i , 67
4	H			1-naphthyl ^c	8j , 45
5	H			4-NMe ₂ C ₆ H ₄ ^c	8k , 47
6	H			4-OMeC ₆ H ₄ ^c	8l , 88
7	Me			Ph ^c	8b , 40
8	Me	6b , 88 ^a	7b , 86	4-NMe ₂ C ₆ H ₄ ^c	8m , 67
9	Me			<i>p</i> -C ₆ H ₄ F ^c	8n , 25
10	F	6c , 53 ^b	7c , 81	Ph ^c	8c , 90
11	CF ₃	6d , 46 ^b	7d , 40	Ph ^d	8d , 92
12	OMe	6e , 65 ^b	7e , 69	Ph ^c	8e , 54
13	Et	6f , 73 ^a	7f , 67	Ph ^c	8f , 74
14	nPr	6g , 80 ^a	7g , 47	Ph ^c	8g , 74

^a Reduction using SnCl₂ in THF, 1M HCl at room temperature 1 hour. ^b Reduction using SnCl₂ in dioxane, BF₃·Et₂O at 105 °C for 20 minutes. ^c Palladium catalyzed cross-coupling using PEPPSI-iPrTM THF at 65 °C. ^d Palladium catalyzed cross-coupling using PEPPSI-iPrTM in toluene at 65 °C.

MATERIAL CHARACTERIZATION

Crystal structure

1
2
3 In small molecule based OPVs exciton dissociation and electron transport generally
4 occurs via Dexter energy transfer.³⁸ For Dexter energy transfer to occur, tight packing and good
5 orbital overlap is required between neighboring molecules in the solid state. Therefore,
6
7 determining the packing in the solid state is critical to understand how a material will function as
8 an organic semiconductor. To examine the solid state packing of ASIs single crystals were
9
10 grown for X-ray diffraction experiments. Single crystals of ASIs were grown as small, purple,
11
12 plate-like crystals via either vacuum sublimation or physical vapor transport using argon as the
13
14 carrier gas.
15
16
17
18
19
20

21 Three packing motifs were observed with ASIs: monoclinic $C2/c$ or $P2_1/c$, and
22 orthorhombic $Pbca$.³⁹ The parent, symmetric compound **8a** packed in the monoclinic $C2/c$ space
23 group.²³ Substitution of hydrogens with isosteric fluorines, as in **8c** and **8h**, also resulted in the
24 same $C2/c$ space group. When larger functional groups were introduced, however, the crystal
25 packing changed to monoclinic $P2_1/c$ for **8d** and **8e**, and orthorhombic $Pbca$ for **8b**.⁴⁰ A range of
26 close contact distances between neighboring molecules was observed in all ASIs due to a slight
27 twisting of the indenotetracene core ranging from 0.70° in **8e**, to 9.67° in compound **8h**. Average
28 π -stacking distances were determined by generating a plane through the ASI molecule using the
29 atoms of the indene ring, supporting information (SI) **Section S3**, and then measuring the
30 distances between neighboring planes. The monoclinic $C2/c$ crystals showed a slipped 1-D
31 packing, **Figure 1a**, with good overlap of the indenotetracene core and small π - π close contacts
32 averaging around 3.4 \AA , (**8a**, **8c**, and **8h**, **Table 2**) which would allow for efficient electron
33 transport.⁴¹ In the solid state compound **8b** (orthorhombic $Pbca$) was observed to pack in a π -
34 stacked herringbone motif, **Figure 1b**. Again, we observed good overlap of the indenotetracene
35 cores with π - π distances that averaged 3.46 \AA and a closest contact measuring 3.36 \AA . In the
36
37
38
39
40
41
42
43
44
45
46
47
48
49
50
51
52
53
54
55
56
57
58
59
60

monoclinic $P2_1/c$ systems, compound **8e** showed little overlap of the indenotetracene core due to a horizontal displacement along the indenotetracene backbone; compound **8d**, however, demonstrated good overlap, **SI Section S3**. Compound **8d** was also unique in that it contained two molecules in the asymmetric unit giving two different π - π close contacts, 3.28 and 3.26 Å. Compounds for which we obtained single crystal X-ray data were further studied for their electrochemical, optical, and physical properties.

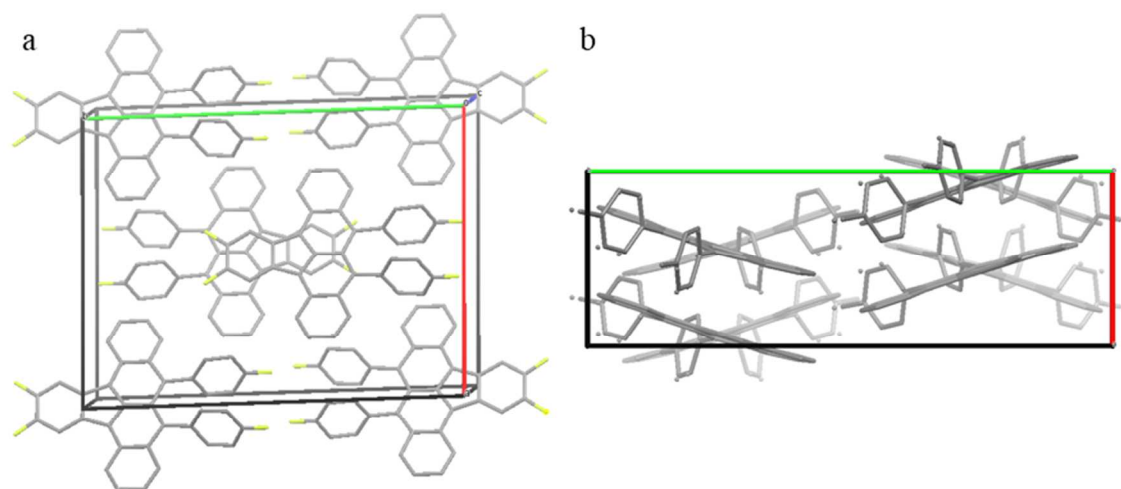


Figure 1: a) $C2/c$ slipped 1-D π -stack in **8c** b) $Pbca$ π -stacked herringbone in **8b** **Table 2:** Single crystal packing motifs for compound **8a–e, h**, and corresponding tetracene backbone π - π distances.

Crystal system	Packing Motif	Compound	π -spacing Å
Monoclinic	$C2/c$	8a	3.42
	$C2/c$	8c	3.42
	$C2/c$	8h	3.37
	$P2_1/c$	8d	3.26/3.28 ^a
Orthorhombic	$P2_1/c$	8e	3.76
	$Pbca$	8b	3.46

^a Compound **8d** contains two molecules in the asymmetric unit with different π - π distances

Thermal Stability

To determine thermal stability and decomposition temperatures, we submitted compounds **8a–e, h** to thermogravimetric analysis (TGA) studies. Shown in **Table S2**,

1
2
3 compounds **8a**, **c**, and **d** demonstrated no more than 1% mass loss below 300 °C, due to
4
5 sublimation, while **8b**, **e**, and **h** did not reach 1 % mass loss until above 300 °C. All ASIs
6
7 demonstrated good thermal stability measuring less than having 5 % mass loss below 325 °C and
8
9 possessing onset temperatures of greater than 343 °C.^{6,42,43} With **8a–e**, **h** demonstrating good
10
11 thermal stability, we next performed differential scanning calorimetry (DSC) to examine phase
12
13 transitions.^{10,15} Complete DSCs for each compound can be found in supporting information
14
15 **Section S3**. The DSC data for compounds **8a–d**, **h** showed no phase change between 0 to 150 °C,
16
17 **Figure 2**. Compound **8e** showed a reversible thermal expansion at 115 °C, **Figure 2**. Upon
18
19 further heating to 260 °C, compounds **8b–e**, **h** showed multiple endothermic events suggesting
20
21 the formation of alternative polymorphs at elevated temperatures. The measured thermal stability
22
23 of ASIs is adequate to resist decomposition or phase changes at typical OPV device operating
24
25 temperatures.
26
27
28
29
30
31
32
33
34
35
36
37
38
39
40
41
42
43
44
45
46
47
48
49
50
51
52
53
54
55
56
57
58
59
60

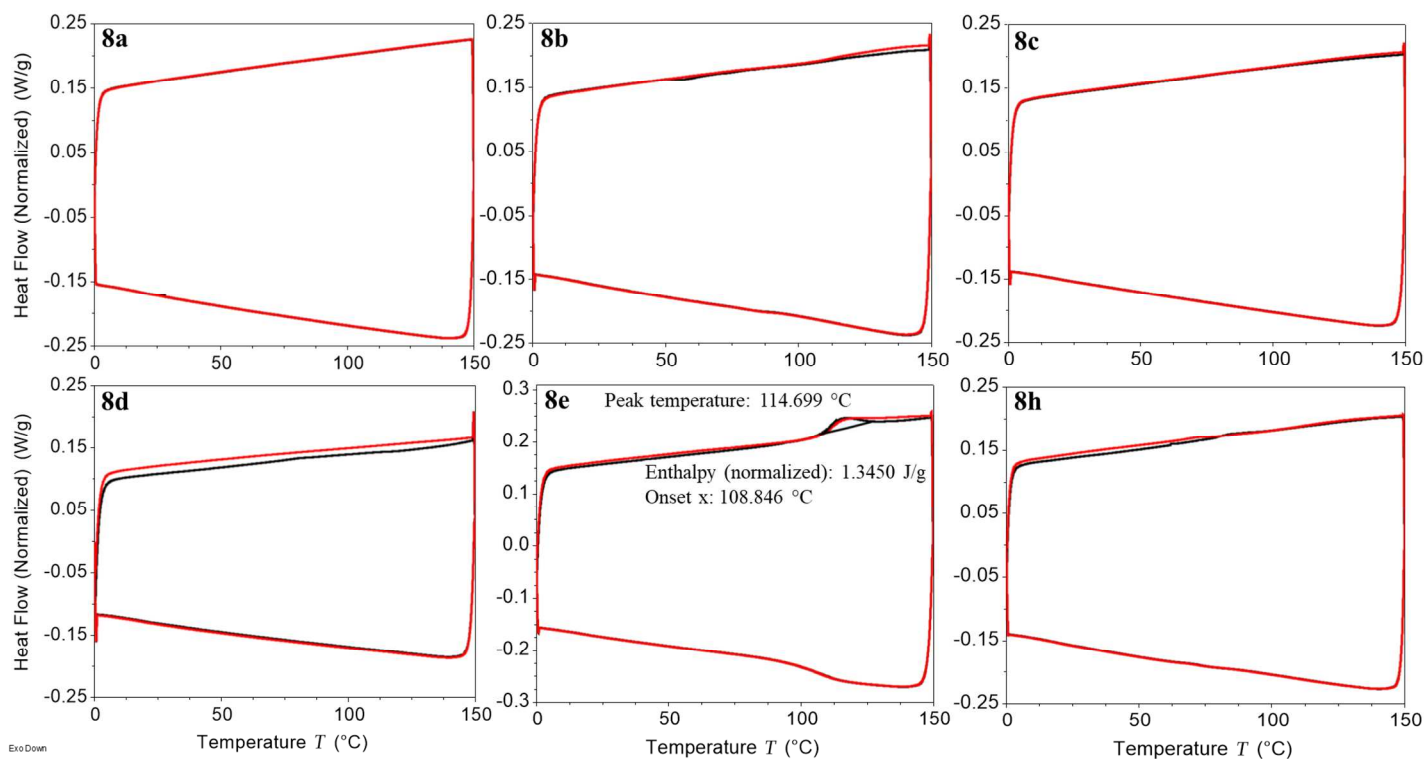


Figure 2: Differential scanning calorimetry results for compounds **8a-e, h**

Electrochemical properties

As stated previously indenotetracenes possess an electron deficient π -system due to the electronic configuration imposed by the five-membered ring. Two-electron reduction has been observed in other indene-containing molecules.^{1,8,44,45} The HOMO and LUMO levels of **8a-e, h**

were determined via cyclic voltammetry (CV) referenced to ferrocene (4.8 eV versus vacuum),

Figure 3. HOMO/LUMO levels were estimated from the onset of the oxidation and reduction peaks, **Section S5**.⁴²

All ASI derivatives showed at least two reversible, or quasi-reversible, reduction and one oxidation red-ox couples. From CV experiments, the energy levels of the LUMO, to which a first electron is added, were determined to be around -4.1 eV while addition of the second electron occurred between -3.27 and -3.42 eV, **Table 3**. The low reduction potentials of ASIs,

1
2
3 $E_{1/2} = -0.9$ to -0.6 V, demonstrate the high electron affinities of these molecules. All ASIs
4
5 showed at least one oxidation peak near $E_{1/2} = 0.7$ V. Estimated HOMO energy levels measured
6
7 for ASIs range from -5.40 to -5.67 eV. The HOMO/LUMO energies determined for ASIs were
8
9 comparable to those determined in other indene-based electron acceptors.^{8,45,46}

10
11
12 We adjusted the HOMO/LUMO energies of ASIs via substitution around the
13
14 indenotetracene core. The addition of an electron donating methoxy group, compound **8e**, raised
15
16 both the HOMO and LUMO in energy. The increased electron density of the indenotetracene
17
18 core raised the HOMO energies to such a degree that a second oxidation peak could now be
19
20 observed, **Figure 3**. Upon addition of CF_3 groups, **8d**, the measured HOMO energy decreased to
21
22 -5.67 eV while addition of the first and second electron into the LUMO lowered to -4.25 and $-$
23
24 3.42 eV respectively. Compound **8d** also now shows a third reduction which occurred at -2.67
25
26 eV. The band gaps calculated from the measured HOMO/LUMO energy levels are shown in
27
28 **Table 3**. The energy gaps determined from CV were found to be in good agreement with the
29
30 calculated energies, **SI Table S16**.

31
32
33 The modulation of HOMO/LUMO levels of ASI via substitution with electron-donating
34
35 and electron-withdrawing groups can be understood by examining the corresponding orbital
36
37 amplitudes (**Figure 4**) determined from density functional theory (DFT) calculation. **Figure 4**
38
39 shows that rather than being localized to one section of the molecule, e.g. the tetracene unit, both
40
41 the HOMO and LUMO are delocalized throughout the entire indenotetracene π -system. The
42
43 HOMO/LUMO energies determined for the ASIs are within the range that would favor electron
44
45 accepting or ambipolar character for charge transport.⁴⁷ The higher LUMO energy levels for
46
47 electron injection into indenotetracenes, compared to that measured for C_{60} , -4.5 eV, would
48
49
50
51
52
53
54
55
56
57
58
59
60

potentially increase the open circuit voltage of an OPV by increasing the difference between the HOMO of the donor and the LUMO of the acceptor.^{48,49,50}

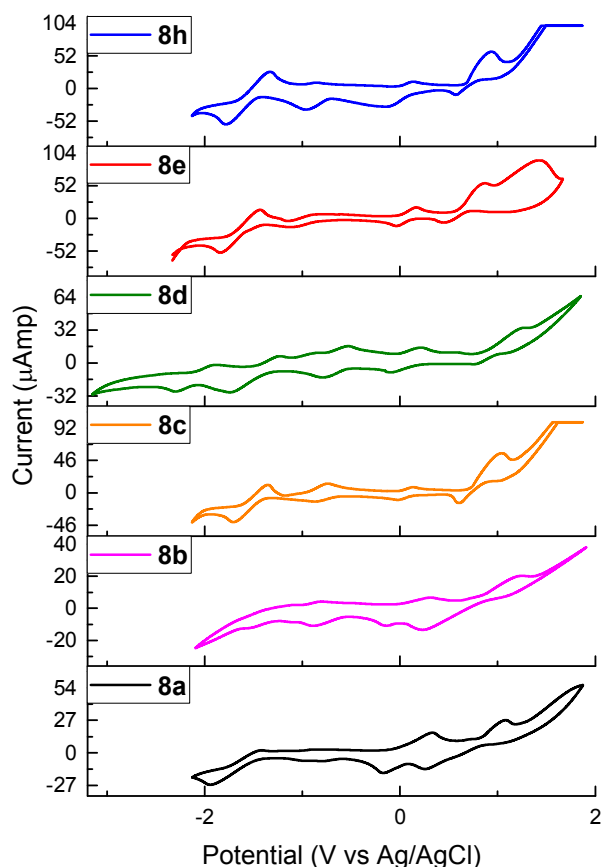


Figure 3: Cyclic voltammogram of compound **8a–e, h**, Fc/Fc⁺ used as standard. Compound **8a, b, d, e** were ran at a scan rate of 0.2 V/s, compound **8c, h** at 0.1 V/s

Table 3: Onset potentials, measured HOMO/LUMO energies for compound **8a–e, h**, compared to Fc/Fc⁺, and energy gap.

Compound	E _{ox/onset} 1 V	E _{red/onset} 1 V	E _{red/onset} 2 V	HOMO eV	LUMO eV	E _g eV	LUMO 2 nd electron eV	E _g eV
8a	0.72	-0.62	-1.47	-5.52	-4.18	1.34	-3.35	2.17
8b	0.74	-0.60	-1.50	-5.54	-4.20	1.34	-3.30	2.24
8c	0.72	-0.65	-1.42	-5.52	-4.15	1.37	-3.38	2.14
8d	0.87	-0.55	-1.38	-5.67	-4.25	1.42	-3.42	2.25
8e	0.60	-0.81	-1.53	-5.40	-3.99	1.41	-3.27	2.13
8h	0.68	-0.65	-1.48	-5.48	-4.15	1.33	-3.32	2.16

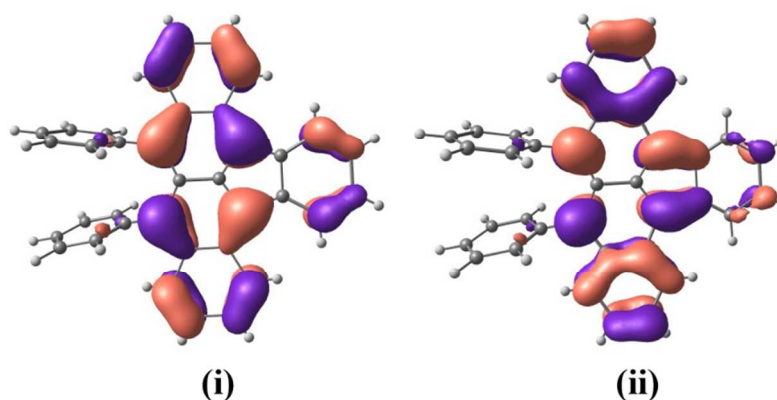


Figure 4. Orbital pictures for i) HOMO and ii) LUMO for **8a** (single point with M06-2X/6-31+G(d,p)).⁵¹

Optical Properties

A major disadvantage of fullerenes is their poor absorptivity of visible light.¹⁴ Having both the donor and acceptor layers being strong absorbers would lead to the creation of more light-generated carriers, increasing short circuit current, improving organic solar cell performance.^{48,49,52}

UV/Visible absorption spectroscopy of compounds **8a–e, h** showed strong absorbance over a large range of the visible spectrum, 390 to 650 nm, **SI Section S7**. All compounds showed very similar absorbance spectra with minor differences in peak shape, **Figure 5**. The variations in peak shape are attributed to the difference in bond vibrational modes/energies and intermolecular interaction between the ASI derivatives. ASIs demonstrated a strong high-energy absorption around 299 nm and weaker mid-range absorption, 350 to 500 nm, which correspond to $\pi-\pi^*$ transitions of the ASI molecules.^{43,53,54} Absorption from 450 to 650 nm is similar to that of other reported indene compounds, resulting from the charge-transfer band, indicating some $\pi-\pi$ interaction between molecules in solution.^{16,20,46} The molar attenuation coefficient determined for compounds **8a–e, h**, **SI Tables S9–S14**, is comparable to ruthenium dipyriddy complexes and

other materials used in dye-sensitized solar cells, which have molar attenuation coefficients around $10^4 \text{ M}^{-1} \text{ cm}^{-1}$ in the visible region.⁵⁵ The energy-gap calculated from the charge-transfer band, λ_{onset} , **Table 4**, for **8a–e, h** were around 1.9 eV. This agrees with those calculated from CV measurements, **Table 3**, and theoretical linear-response time-dependent density functional theory (LR-TDDFT) calculations, **Table S16**.

Comparing the absorbance of ASIs molecules to symmetrically substituted indenotetracenes we observed that both have similar molar attenuation coefficients, between 10^4 and $10^5 \text{ M}^{-1} \text{ cm}^{-1}$. This is to be expected due to the fact that π -conjugation of the indenotetracene core are same.²³

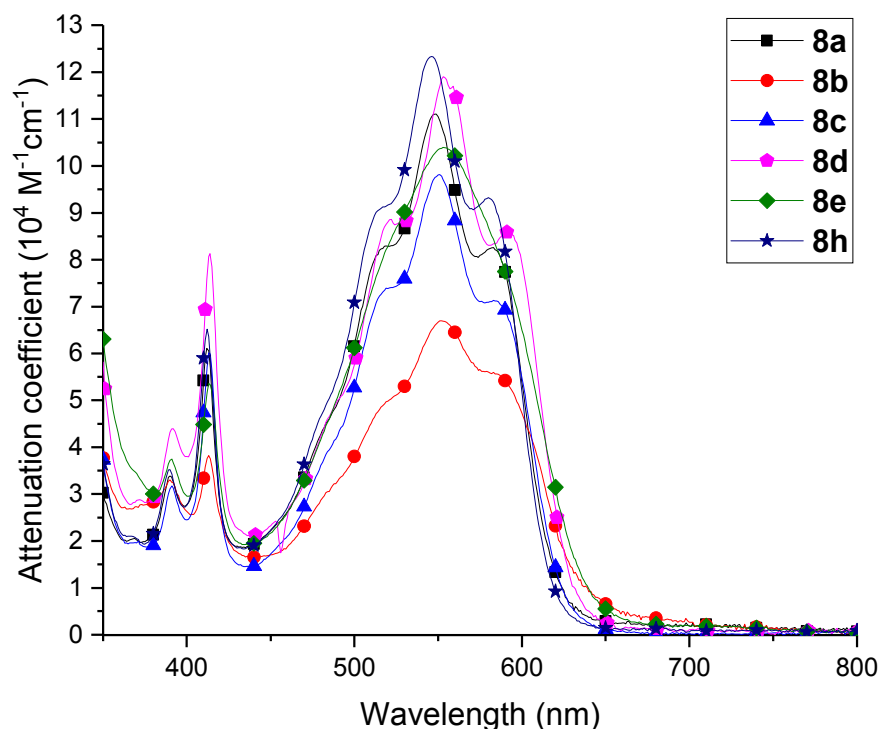


Figure 5: Absorption spectra of compounds **8a–e, h**, 10^{-5} M

Table 4: λ_{max} and optical band gaps

Compound	λ_{max} (nm)	E_g (eV) ^a
----------	--------------------------------	-------------------------

8a	550	1.98
8b	553	1.86
8c	551	1.93
8e	553	1.96
8d	555	1.89
8h	546	1.98

^a Optical band gap was calculated using equation $E_g = \frac{hc}{\lambda}$ where h is Planck's constant, c is the speed of light constant, and λ is the absorption onset.

Fluorescence is the most common path for exciton decay in organic materials, and can decrease OPV efficiency by decreasing exciton (Dexter) energy transfer. **Figure 6** shows the absorbance and corresponding fluorescence spectra of compounds **8a-e, h**. Derivatives **8a-e, h** demonstrated weak fluorescence from 600 to 800 nm, which is common for similar, indene-containing molecules.⁸ The fluorescence quantum yields for compounds **8a-e** and **h**, **Table 5**, were all less than 4 %.

A portion of the very low Φ can be attributed to re-absorbance due to partial overlap of the absorption and fluorescence spectra. The lack of any significant fluorescence indicates that non-radiative decay pathways, which may include intersystem crossing and/or intermolecular charge transfer, are occurring.^{6,54,56} If operative, these alternate decay pathways could increase the efficiency of OPVs in which ASIs are used as the electron accepting layer due to the possible generation of longer lived excitons as well as faster exciton dissociation.^{10,15,57}

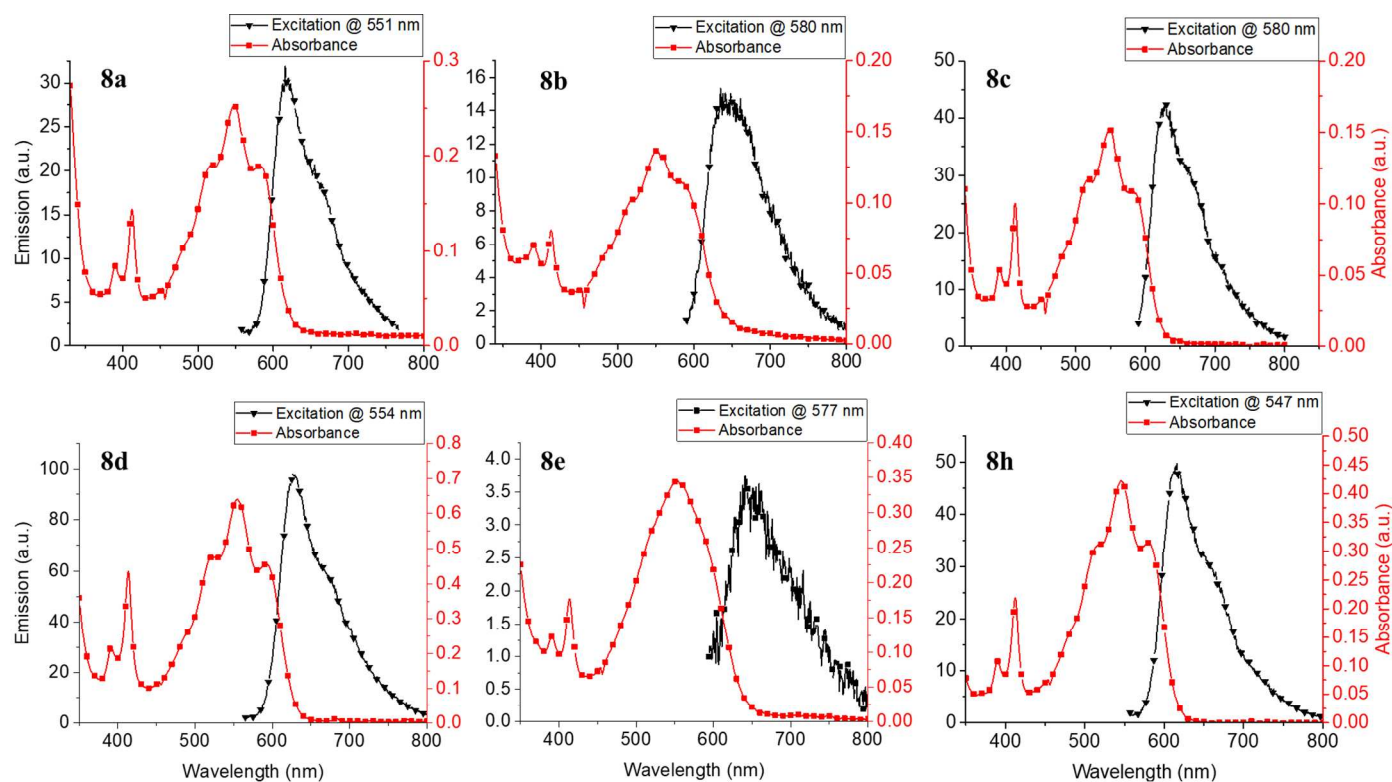


Figure 6: Fluorescence and corresponding absorbance spectra compounds **8a-e, h**.

Table 5: Calculated fluorescence quantum yield for compounds **8a-e, h** relative to rhodamine b.

Compound	Φ
Rhodamine B	0.7
8a	0.018
8b	0.016
8c	0.042
8d	0.029
8e	0.0015
8h	0.018

Theoretical modeling of electronic structure of ASI and charge transport in the solid state

To understand excited-state properties of ASIs, LR-TDDFT calculations were performed. As stated previously, the LR-TDDFT calculations for singlet and triplet energies agreed well with those determined experimentally. Singlet-triplet energy gaps in ASIs also suggest the possibility of singlet fission occurring in these molecules. Singlet fission is a process where one singlet exciton is converted into two triplet excitons in a spin allowed process. For singlet fission

1
2
3 to occur, transition from the singlet excited state to the multiexcitonic state with two correlated
4 triplet excitons must be exoergic or at least isoergic, $E_S \geq 2E_T$. For compound **8a** $E_S - 2E_T$ is
5 0.1 eV, 0.96 kJ/mol. The same relationship was also found for compounds **8b-e, h**, **Table S16**.⁵⁸
6
7 Singlet fission has been observed in other acenes and is thought to be highly beneficial for
8 increasing the efficiency of OPVs.⁵⁹⁻⁶¹
9
10
11
12
13

14 The hole and electron reorganization energies were computed for ASI derivatives **8a-e, h**
15 and found to be comparable (see SI).⁶² For each compound, **8a-d, h**, the hole reorganization
16 energy was found to be slightly smaller than the electron reorganization energy, except for **8e**.
17 The presence of the methoxy group in **8e** significantly increased the hole reorganization energy
18 compared to **8a-d, h**, while leaving the electron reorganization energy unchanged.
19
20
21
22
23
24
25

26 Hole and electron transfer integrals were computed for compounds **8a-e, h** using dimer
27 models developed from the solved single-crystal X-ray structures of each compound (**Table 6**;
28 see SI **Section S2** for dimer pictures). For compounds **8a** and **h**, C2/c crystal structures with 1-D
29 brick packing, the electron transfer integral was determined to be significantly higher than the
30 hole transfer integral. However, in the case of compound **8c**, also C2/c and 1-D brick packing,
31 the hole and electron transfer integrals were comparable. Compound **8b**, with Pbc_a packing, had
32 an absolute electron transfer integral significantly higher than the hole transfer integral. The
33 P2₁/c crystal system gave two very different results depending on the substitution. Methoxy-
34 substituted ASI **8e** had a hole transfer integral 3 times larger than the electron transfer integral;
35 however, CF₃-substituted ASI **8d** had comparable hole and electron transfer integrals.
36
37
38
39
40
41
42
43
44
45
46
47
48

49 Calculated electron transfer integrals for perylene diimides, a proven small molecule
50 electron transport material, range from 10 to 200 meV depending on the functional group and the
51 model used.^{63,64} The computed transfer integrals for **8a-d, h** were found to be comparable to
52
53
54
55
56
57
58
59
60

those observed for perylene diimides. When considering both the reorganization energies and charge transfer integrals, theoretical calculations predict that compounds **8a–d**, **h** could function as either an electron transport or ambipolar material allowing them to function as n-type semiconductors in OPVs.

Table 6: Absolute values for effective transfer integral (meV, PBE0/6-31G(d)) predicted for compounds **8a–e**, **h**.⁶⁵

Compounds	Crystal Packing	Transfer integrals Electron (meV)	Transfer integrals Hole (meV)
8a	C2/c	32	5
8b	Pbca	34	4
8c	C2/c	19	28
8d	P2 ₁ /c	87/53 ^a	82/81 ^a
8e	P2 ₁ /c	19	57
8h	C2/c	44	7

^a Compound **8d** contains two molecules in the asymmetric unit with slightly different π – π distances. Transfer integrals were calculated for both distances

Conclusion

In summary, a new class of electron transport material based on the indene scaffold, asymmetrically substituted indenotetracenes (ASI), have been successfully prepared. Electrochemical and thermal characterizations demonstrate the potential of ASIs as a novel electron transport material in OPVs. ASIs were shown to strongly absorb over a broad range of the visible spectrum, with little to no concomitant fluorescence, potentially increasing short circuit current. The higher LUMO levels of ASIs relative to C₆₀ should allow for increased open circuit voltage. ASIs also demonstrated good thermal stability which could improve OPV lifetime. Single crystal X-ray diffraction experiments showed tight π -stacking and good backbone overlap in the solid state, allowing for efficient charge transport in the solid state.

Using the solved crystal structure, ASIs were predicted to have either electron transport or ambipolar character in organic photovoltaic devices.

Our findings demonstrate the potential of asymmetrically substituted indenotetracenes to function as a novel class of non-fullerene electron transport materials in organic photovoltaics with the potential to improve device lifetime and efficiency.

EXPERIMENTAL SECTION

Materials and reagents

All materials were purchased through commercial sources. THF was distilled from sodium and benzophenone. Toluene was distilled from CaH_2 . 2-(1-hydroxy-2-naphthoyl)benzoic acid (**3**) and 6-chlorotetracene-5,12-dione (**4**) were synthesized using a previously published procedure.⁹

Measurements and characterization

Melting temperatures for all compounds were performed on samples precipitated from solution.

The melting temperature is defined as the temperature at which the powder anneals to a film rather than a free-flowing liquid. High-resolution mass spectrometry (HRMS) using GC-MS was performed on a quadrupole time-of-flight mass spectrometer with a solid injection probe.

Method: inlet temperature 250 °C, source temperature 280 °C. The initial temperature was 80 °C and increased to 325 °C over 6 minutes and then held for 2.3 minutes. High-resolution mass spectrometry (HRMS) using ESI was performed on time-of-flight instruments.

^1H NMR (300, 400, or 500 MHz), and ^{13}C NMR (75, 100, or 125 MHz), ^{19}F NMR (282 or 470 MHz) spectra were recorded on FT NMR instruments. All NMR spectra were reported as δ values in ppm referenced to chloroform (7.26 ppm), methylene chloride (5.32 ppm) or tetramethylsilane (TMS, 0.00 ppm) for ^1H , chloroform (77.00 ppm) for ^{13}C , and

1
2
3 hexafluorobenzene (-163.00 ppm) for ^{19}F NMR. ^{13}C NMR spectra are reported to the nearest
4
5 0.01 ppm due to the large number of close signals.
6

7
8 Infrared (IR) spectra were obtained as films on NaCl plates using an infrared spectrophotometer
9
10 in transmission mode.
11

12 X-ray diffraction experiments were performed via single-crystal XRD using a diffractometer
13
14 with graphite monochromator using $\text{CuK}\alpha$ radiation ($\lambda=1.5418$) at 123 K ω scans and $\text{MoK}\alpha$
15
16 radiation ($\lambda=0.71073$) at 298 K ω scans. Crystals of **8a**, **d**, **c**, and **h** were grown via physical
17
18 vapor transport (PVT) using the following technique: the temperature of the sublimation region
19
20 was adjusted for each compound and ranged between 150 and 230 °C, depending on the
21
22 compound. The crystal growth was held between 140 and 200 °C. The thermal gradient in the
23
24 crystal growth region was created by wrapping thermal tape at continually wider intervals down
25
26 the crystal growth region. Argon was used as the carrier gas. Argon flow rate was set via an oil
27
28 bubbler at one bubble in the oil bubbler every 1 to 2 seconds. The crystals were grown in the
29
30 PVT chamber over a 1 to 3 day period. Crystals of **8b**, **c** were grown via sublimation between
31
32 180 and 200 °C over 3 days under high vacuum. In the solid state, compounds **8a-c**, and **h** are
33
34 configurationally disordered resulting in having to place the substitutions symmetrically about
35
36 the diarylindenotetracene core with 50 % occupancy.
37
38
39
40
41

42 Differential scanning calorimetry experiments were performed by heating compounds **8a-e**, **h** to
43
44 150 °C at 10 °C/ min for two cycles then heating to 260 °C in a differential scanning calorimeter.
45
46 Thermogravimetric analysis was performed by heating samples from 24 to 550 °C at a rate of 10
47
48 °C/ minute in a nitrogen atmosphere.
49
50

51 Cyclic voltammetry measurements were performed at 5 mM in anhydrous tetrahydrofuran
52
53 previously degassed with Argon. A silver/silver chloride reference electrode, gold working
54
55
56
57
58
59
60

1
2
3 electrode, and platinum ground were used for CV experiments. Tetrabutylammonium perchlorate
4 was used as the electrolyte and ferrocene as the standard. Cyclic voltamograms were collected at
5
6 varying concentrations and sweep rates with all showing similar Red/Ox character. Ferrocene
7
8 oxidation onset was referenced to zero.
9

10
11 Absorbance measurements were performed on a UV/Visible spectrometer, scanned from
12
13 1000nm to 100nm as follows: indenotetracene compounds **8a-e, h** were dissolved in
14
15 dichloromethane (10 mL). Serial dilutions were performed in factor of ten increments (10^{-3} , 10^{-4} ,
16
17 10^{-5} , 10^{-6} M) and absorbance was measured. Serial dilutions were performed using a 10 mL
18
19 volumetric flask and 1 mL volumetric pipet. Attenuation coefficients (ϵ) were calculated from
20
21 absorbance spectra corrected for dichloromethane.
22
23

24
25 Fluorescence experiments were performed on a fluorescence spectrophotometer in either ethanol
26
27 or dichloromethane. The fluorescence quantum yield was calculated using rhodamine b in
28
29 ethanol excited at 510 nm. The quantum yield for rhodamine b under these conditions was
30
31 previously reported, $\Phi = 0.7$.^{66,67} Absorption and fluorescence measurements for compounds **8 a-**
32
33 **e and h** were performed at 10^{-5} M
34
35

36 37 **Computational Methodology:**

38
39 **Monomer:** We optimized monomer geometries for neutral, radical cation, and anion species in
40
41 the gas phase using the M06-L exchange-correlation and 6-31+G(d,p) basis set.⁵¹ Vibrational
42
43 frequency analyses were done to confirm that all structures are minima. LR-TDDFT calculations
44
45 are performed on neutral optimized geometries in the gas phase using the M06-2X exchange-
46
47 correlation functional and 6-31+G(d,p) basis set.
48
49

50
51 **Dimer:** We used dimer models to elucidate the transfer of holes and electrons through the
52
53 specific packing arrangements of different diarylindenotetracene derivatives. We extracted dimer
54
55
56
57
58
59
60

1
2
3 models from experimental crystal structures of different diarylindenotetracene derivatives.
4
5 Subsequently, we constrained the backbone of the diarylindenotetracene derivatives and
6
7 optimized periphery aryl groups and the substituents. It is important to perform these constrained
8
9 optimizations as there are often uncertainties in the crystal structures related to the position of
10
11 the periphery aryl group and the substituents. Constrained optimization of dimers was
12
13 performed using the PBE functional and 6-31G(d,p) basis set.⁶⁸ Damped dispersion effects
14
15 were included with the pairwise D3 correction of Grimme et al. and the damping function of
16
17 Becke and Johnson.
18
19

20
21
22 Optimized dimer geometries were used to calculate charge transfer integrals were
23
24 accomplished using PBE0/6-31G(d) level of theory and the fragment molecular orbital (FMO)
25
26 approach. In the FMO approach, a dimer Fock matrix is constructed in the basis of monomer
27
28 orbitals. Off-diagonal elements of the Fock matrix are $t_{mn} = \langle \varphi_m | h_{KS} | \varphi_n \rangle$, where φ_i represents
29
30 the fragment molecular orbitals and i represents the sites (m or n). For the matrix elements
31
32 relevant to the hole (or the electron) transfer integral between the m^{th} and n^{th} sites in a system,
33
34 φ_m and φ_n are the HOMOs (or LUMOs) of m^{th} and n^{th} site respectively. Here, as we are using a
35
36 dimer model, sites represent individual monomers and h_{KS} is the Kohn-Sham Fock operator.
37
38 Diagonal elements of the Fock matrix are site energies, $\varepsilon_i = \langle \varphi_i | h_{KS} | \varphi_i \rangle$. S_{mn} is the overlap
39
40 matrix element between orbital φ_m and φ_n . Since the Fock matrix is constructed here by using
41
42 nonorthogonal monomer orbital basis, effective transfer integral (t_{mn}^{eff}) is calculated using the
43
44 formula,
45
46
47
48
49

$$t_{mn}^{\text{eff}} = \frac{t_{mn} - \frac{1}{2}(\varepsilon_m + \varepsilon_n)S_{mn}}{1 - S_{mn}^2} \quad (1)$$

50
51
52
53
54
55
56
57
58
59
60

1
2
3 All optimization of monomers and dimers and LR-TDDFT calculations were performed using
4 *Gaussian09* software.⁶⁹ Transfer integral calculations are performed using a developer version
5 of *NWChem*.⁷⁰
6
7

8 9 10 **Synthesis**

11 12 **6-Chloro-5,12-diphenyl-5,12-dihydrotetracene-5,12-diol (5a):**

13
14 To a flame-dried 250 mL round-bottom flask, bromobenzene (3.23 mL, 30.8 mmol) and 30 mL
15 anhydrous tetrahydrofuran (THF) were added under nitrogen. The solution was cooled to $-78\text{ }^{\circ}\text{C}$
16 and then *tert*-butyllithium (1.7 M, 36.2 mL, 61.5 mmol) was added dropwise to the stirring
17 solution. The slurry was stirred at $-78\text{ }^{\circ}\text{C}$ for 1 h, then warmed to $0\text{ }^{\circ}\text{C}$ and the resultant
18 phenyllithium was used immediately. To a flame-dried 500 mL round-bottom flask, 6-chloro-
19 5,12-naphthacenequinone **4** (1.50 g, 5.12 mmol) and 150 mL anhydrous THF were added under
20 nitrogen. The suspension was cooled to $-78\text{ }^{\circ}\text{C}$ and the solution of phenyllithium, prepared
21 earlier, was added slowly. The suspension turned green and became a homogeneous solution
22 upon the completion of addition. The solution was stirred at $-78\text{ }^{\circ}\text{C}$ for 1 h then warmed to
23 room temperature and stirred for 14 h. The reaction was quenched with 1 N HCl (100 mL) and
24 extracted with EtOAc ($2 \times 50\text{ mL}$). The organic layers were combined, washed sequentially with
25 saturated NaHCO_3 (50 mL) and brine (20 mL), dried over anhydrous Na_2SO_4 , and concentrated
26 under vacuum. The crude product was carried forward without further purification.
27
28
29
30
31
32
33
34
35
36
37
38
39
40
41
42
43

44 45 **5-Chloro-6,11-diphenyltetracene (6a):**

46
47 The resultant residue, compound **5a**, was dissolved in 15 mL THF. To the resulting saturated
48 solution of SnCl_2 (6.80 g, 35.9 mmol) in conc. HCl (approximately 10 mL) was added slowly, a
49 red solid precipitated upon addition. The slurry was stirred for additional 1 h upon complete
50 addition of SnCl_2 . The reaction was quenched by pouring the slurry into H_2O (200 mL). The red
51
52
53
54
55
56
57
58
59
60

1
2
3 solid was collected by vacuum filtration. The filtrate was recrystallized from a hot solution of
4
5 toluene/isopropanol (1:10) to give **6a**, a red/orange solid (1.70 g, 4.10 mmol, 80%): mp 188-189
6
7 °C; ¹H NMR (300 MHz, CDCl₃) δ 8.38 (d, *J* = 9.1 Hz, 1H), 8.32 (s, 1H), 7.75 (d, *J* = 8.5 Hz,
8
9 1H), 7.71–7.58 (m, 5H), 7.57–7.50 (m, 5H), 7.50–7.39 (m, 3H), 7.36–7.29 (m, 1H), 7.28–7.22
10
11 (m, 2H); ¹³C NMR (75 MHz, CDCl₃) δ 142.1, 139.3, 138.2, 136.0, 131.8, 131.5, 131.4, 130.6,
12
13 130.1, 130.0, 129.2, 128.8, 128.6, 127.8, 127.7, 127.4, 127.0, 126.8, 126.5, 125.2, 125.1, 125.0
14
15 (Not all carbon signals are resolved); IR (KBr) ν 3040, 1598, 1387, 1361, 1238 cm⁻¹; HRMS
16
17 (ESI-TOF) *m/z*: [M]⁺ Calcd for C₃₀H₁₉Cl 414.1175; found 414.1171.

21 22 **9-Chloro-10-phenylindeno[1,2,3-*fg*]tetracene (7a):**

23
24 To a flame-dried 100 mL round-bottom flask, anhydrous aluminum chloride (1.60g, 12.1 mmol)
25
26 and 15 mL freshly distilled nitrobenzene was added under nitrogen. The slurry was stirred at 60
27
28 °C for ten minutes and formed a clear solution. To the solution, compound **6a** (1.00 g, 2.41
29
30 mmol) and additional nitrobenzene (5 mL) were added. The reaction turned dark green upon the
31
32 completion of addition. The reaction was stirred at 60 °C for 3 to 4 h and allowed to cool to
33
34 room temperature. The dark green solution was then poured onto a mixture of ice and 1N HCl
35
36 solution, turning purple instantaneously. The mixture was extracted with EtOAc (2 × 50 mL).
37
38 The organic layers were combined, filtered and concentrated under vacuum. The remaining
39
40 nitrobenzene was subsequently removed by azeotropic distillation with H₂O (150 mL). The
41
42 residue was collected and recrystallized from hot toluene (first crop) and DCM/MeOH (second
43
44 crop) to give **7a**, a purple/black solid (811 mg, 1.96 mmol, 81%): mp 262–263 °C; ¹H NMR (300
45
46 MHz, CDCl₃) δ 8.87 (dd, *J* = 8.2, 6.9 Hz, 2H), 8.61–8.47 (m, 3H), 7.70 (d, *J* = 9.1 Hz, 1H), 7.68–
47
48 7.59 (m, 2H), 7.58–7.55 (m, 3H), 7.53–7.41 (m, 5H), 7.33 (ddd, *J* = 1.0, 6.5, 9.2 Hz, 1H); IR
49
50 (KBr) ν 3068, 3027, 1597, 1451, 1380, 1276, 1150 cm⁻¹; HRMS (ESI-TOF) *m/z*: [M]⁺ Calcd for
51
52
53
54
55
56
57
58
59
60

C₃₀H₁₇Cl 412.1019; found 412.0990. A suitable ¹³C NMR spectrum could not be obtained due to poor solubility.

9,10-Diphenylindeno[1,2,3-*fg*]tetracene (8a):

To a flame-dried 100 mL round-bottom flask, compound **7a** (100 mg, 0.242 mmol), PEPPSI-IPr (16.0 mg, 0.0235 mmol) and 10 mL freshly distilled 1,4-dioxane were added. The flask was then sealed with a septum and placed under a nitrogen atmosphere. The solution was stirred at room temperature and phenylmagnesium bromide in THF (0.24 M, 10 mL, 2.42 mmol) was added. The reaction was heated to 60 °C and stirred for 4 h. The reaction was then quenched with 1N HCl and extracted with EtOAc (2 × 50 mL). The organic layers were combined, dried over Na₂SO₄ and concentrated under vacuum. The residue was purified by flash column chromatography (silica gel, 5% ethyl acetate in hexanes, R_f = 0.30) to give **8a** (87.5 mg, 0.192 mmol, 80%). In order to obtain the product in a solid form, the product obtained from chromatography was purified by recrystallization in DCM/MeOH to give **8a**, a purple/black solid (65.1 mg, 0.143 mmol, 60%): mp 271–272 °C; ¹H NMR (300 MHz, CDCl₃) δ 8.93 (d, *J* = 8.8 Hz, 2H), 8.61 (dd, *J* = 5.6, 3.2 Hz, 2H), 7.59 (m, 2H), 7.53 (dd, *J* = 5.6, 2.8 Hz, 2H), 7.36 (d, *J* = 9.2 Hz, 2H), 7.21 (ddd, *J* = 7.2, 6.4, 0.8 Hz, 2H), 7.05 (m, 6H), 6.93 (m, 4H); ¹³C NMR (75 MHz, CDCl₃) δ 140.8, 140.2, 139.7, 134.0, 131.6, 131.0, 129.2, 128.9, 128.2, 127.4, 127.2, 126.7, 126.3, 124.4, 124.2, 123.8 (not all carbon signal were resolved); IR (thin film) ν 3055, 1946, 1598, 1552, 1449, 1441, 1396, 1361 cm⁻¹; HRMS (ESI-TOF) *m/z*: [M+H]⁺ Calcd for C₃₆H₂₃ 455.1800; found 455.1806.

6-Chloro-5,12-di-*p*-tolyl-5,12-dihydrotetracene-5,12-diol (5b):

6-chloro-5,12-di-*p*-tolyl-5,12-dihydrotetracene-5,12-diol was synthesized analogously to 6-chloro-5,12-diphenyl-5,12-dihydrotetracene-5,12-diol, compound **5a**. The crude product was carried to the next step without purification.

5-Chloro-6,11-di-*p*-tolyltetracene (6b):

5-chloro-6,11-di-*p*-tolyltetracene was synthesized analogously to 5-chloro-6,11-diphenyltetracene, compound **6a**, to give an red/orange solid (2.00 g, 4.51 mmol, 88%): mp 197–198 °C; ¹H NMR (300 MHz, CDCl₃) δ 8.39 (d, *J* = 9.1 Hz, 1H), 8.35 (s, 1H), 7.76 (d, *J* = 8.1 Hz, 1H), 7.70–7.59 (m, 2H), 7.49–7.37 (m, 5H), 7.35 (s, 4H), 7.30 (d, *J* = 6.5 Hz, 1H), 7.27–7.24 (dd, *J* = 5.6, 1.9 Hz, 2H), 2.59 (s, 3H), 2.56 (s, 3H); ¹³C NMR (75 MHz, CDCl₃) δ 139.1, 138.1, 137.4, 136.6, 136.2, 136.0, 132.0, 131.3, 130.5, 130.2, 130.1, 129.3, 128.8, 128.6, 128.4, 127.5, 126.9, 126.9, 126.6, 125.7, 125.3, 125.0, 125.0, 21.5, 21.5 (Not all carbon signals are resolved); IR (KBr) ν 3043, 3016, 2864, 2857, 1510, 1459, 1387, 1357 cm⁻¹; HRMS (ESI-TOF) *m/z*: [M]⁺ Calcd for C₃₂H₂₃Cl 442.1488; found 442.1488.

10-Chloro-2-methyl-9-(*p*-tolyl)indeno[1,2,3-*fg*]tetracene (7b):

10-chloro-2-methyl-9-(*p*-tolyl)indeno[1,2,3-*fg*]tetracene was synthesized analogously to 9-chloro-10-phenylindeno[1,2,3-*fg*]tetracene, compound **7a**, to give an purple solid (680 mg, 1.54 mmol, 86%): mp 197–198 °C; ¹H NMR (300 MHz, CDCl₃) δ 8.39 (d, *J* = 9.1 Hz, 1H), 8.35 (s, 1H), 7.76 (d, *J* = 8.4 Hz, 1H), 7.71–7.58 (m, 2H), 7.50–7.37 (m, 5H), 7.35 (s, 3H), 7.30 (d, *J* = 6.5 Hz, 1H), 7.23 (d, *J* = 3.0 Hz, 1H), 2.59 (s, 3H), 2.56 (s, 3H); ¹³C NMR (75 MHz, CDCl₃) δ 139.1, 138.1, 137.4, 136.6, 136.2, 136.0, 132.0, 131.3, 130.5, 130.2, 130.1, 129.3, 128.8, 128.6, 128.4, 127.5, 126.9, 126.9, 126.6, 125.7, 125.3, 125.0, 125.0, 21.5, 21.5 (not all carbon signals are resolved); IR (KBr) ν 3023, 2915, 1686, 1601, 1557, 1511, 1458, 1431, 1392, 1377, 1304 cm⁻¹; HRMS (ESI-TOF) *m/z*: [M]⁺ Calcd for C₃₂H₃₂Cl 440.1332; found 440.1325.

2-Methyl-10-phenyl-9-(*p*-tolyl)indeno[1,2,3-*fg*]tetracene (8b)

To a flame-dried 100 mL round-bottom flask, **7b** (400 mg, 0.907 mmol), PEPPSI-IPr (31.0 mg, 0.0456 mmol) and 10 mL freshly distilled 1,4-dioxane were added. The flask was then sealed with a septum and placed under a nitrogen atmosphere. The solution was stirred at room temperature and phenylmagnesium bromide in THF (0.910 M, 10 mL, 9.10 mmol) was added. The reaction was heated to 60 °C and stirred for 4 h. The reaction was then quenched with 1N HCl and extracted with EtOAc (2 × 50 mL). The organic layers were combined, dried over Na₂SO₄ and concentrated under vacuum. The residue was purified by flash column chromatography (silica gel, 5% ethyl acetate in hexanes, R_f=0.40) to give **8b** (387 mg, 0.802 mmol, 88%). In order to obtain the product in a solid form, the product obtained from chromatography was purified by recrystallization from hot toluene/*i*PrOH (1:10) to give a purple/black solid, compound **8b** (175 mg, 0.363 mmol, 40%): mp 179–180 °C; ¹H NMR (300 MHz, CDCl₃) δ 8.89 (dd, *J* = 8.9, 15.9 Hz, 2H), 8.45 (d, *J* = 7.9 Hz, 1H), 8.40 (s, 1H), 7.62–7.53 (m, 2H), 7.45 (d, *J* = 9.1 Hz, 1H), 7.34 (dd, *J* = 11.9, 6.7 Hz, 2H), 7.20 (dd, *J* = 9.2, 6.4 Hz, 2H), 7.14 (dd, *J* = 8.3, 6.4 Hz, 1H), 7.03 (t, *J* = 7.4 Hz, 2H), 6.90 (dd, *J* = 5.2, 3.1 Hz, 2H), 6.84–6.76 (m, 4H), 2.64 (s, 3H), 2.32 (s, 3H); ¹³C NMR (75 MHz, CDCl₃) δ 140.7, 140.4, 140.1, 137.2, 137.1, 136.4, 135.5, 134.0, 133.9, 131.6, 131.5, 131.1, 129.3, 129.3, 128.8, 128.5, 128.4, 127.8, 127.4, 127.2, 127.2, 127.0, 125.5, 125.2, 124.6, 124.3, 123.9, 123.8, 22.1, 21.2. (Not all carbon signals are resolved); IR (KBr) ν 3042, 3021, 2912, 2857, 1599, 1558, 1511, 1456, 1434, 1396, 1360, 1294, 1133, 1021 cm⁻¹; HRMS (ESI-TOF) *m/z*: [M]⁺ Calcd for C₃₈H₂₆ 482.2035; found 482.2026.

6-Chloro-5,12-bis(4-fluorophenyl)-5,12-dihydro-tetracene-5,12-diol (5c):

1
2
3 To a flame dried 100 mL 3-neck round bottom flask was added anhydrous THF (50 mL), which
4 was cooled to $-77\text{ }^{\circ}\text{C}$. 1-bromo-4-fluorobenzene (1.965 mL, 3.130 g, 17.89 mmol) was added to
5 THF at $-77\text{ }^{\circ}\text{C}$ followed by n-butyllithium (2.5 M in hexane, 6.439 mL, 24.53 mmol). The
6 mixture was stirred at $-77\text{ }^{\circ}\text{C}$ for 10 minutes to form 4-fluorophenyllitium. In a flame dried 250
7 mL 3-neck round bottom flask anhydrous THF (150 mL) and 6-chloro-5,12-naphthacenequinone
8 **4** were combined and cooled to $-77\text{ }^{\circ}\text{C}$. The 4-fluorophenyllitium was transferred into the 250
9 mL round bottom containing the slurry of THF and 6-chloro-5,12-naphthacenequinone via
10 cannula at a constant flow. The mixture was allowed to react at $-77\text{ }^{\circ}\text{C}$ for 2 hours then allowed
11 to warm to room temperature and stirred for an additional hour. The reaction was quenched with
12 water (2 mL). The crude reaction mixture was concentrated to a solid and carried forward
13 without purification.
14
15
16
17
18
19
20
21
22
23
24
25
26
27

28 **5-Chloro-6,11-bis(4-fluorophenyl)tetracene (6c):**

29
30 The crude reaction mixture of compound **5c** was dissolved in 100 mL of dioxane and poured into
31 a 250 mL round bottom flask. Tin (II) chloride (5.652 g, 29.81 mmol) and $\text{BF}_3\cdot\text{OEt}_2$ (2.207 mL,
32 2.538 g, 17.89 mmol) were added to the 250 mL round bottom. The reaction mixture was heated
33 to reflux ($106\text{ }^{\circ}\text{C}$) and reflux was maintained for 45 minutes. The reaction mixture was then
34 allowed to cool to room temperature and quenched with saturated aqueous NaHCO_3 solution,
35 followed by addition of solid NaHCO_3 until the aqueous portion is basic as indicated by pH
36 paper. The precipitate that formed was removed via filtration over Celite. The filtered solid was
37 washed with chloroform ($3 \times 250\text{ mL}$). The filtrate and chloroform washes were combined and
38 washed once with water, once with saturated brine, dried over MgSO_4 , concentrated and placed
39 under high vacuum overnight. The crude product was dissolved in boiling chloroform followed
40 by the addition of room temperature methanol and placed in the refrigerator ($5\text{ }^{\circ}\text{C}$) overnight.
41
42
43
44
45
46
47
48
49
50
51
52
53
54
55
56
57
58
59
60

This gave compound **6c**, an orange/red solid (2 steps 1.425 g, 3.160 mmol, 53%): mp 207–208 °C; ¹H NMR (500 MHz CDCl₃) δ 8.40 (d, *J* = 9.1 Hz, 1H), 8.28 (s, 1H), 7.77 (d, *J* = 8.6 Hz, 1H), 7.66–7.60 (m, 1H), 7.60–7.55 (m, 1H), 7.50–7.47 (m, 3H), 7.45–7.34 (m, 6H), 7.30–7.27 (m, 2H), 7.25–7.23 (m, 1H); ¹³C NMR (126 MHz CDCl₃) δ 163.5 (d, *J* = 21.8 Hz), 161.5 (d, *J* = 20.7 Hz), 137.8 (d, *J* = 3.6 Hz), 137.2, 135.1, 135.0 (d, *J* = 3.6 Hz), 133.0 (d, *J* = 7.9 Hz), 132.9 (d, *J* = 7.8 Hz), 132.0, 130.8, 130.3, 130.2, 129.4, 128.8, 128.6, 127.3 (d, *J* = 6.8 Hz), 126.6, 126.3, 125.7, 125.6, 125.5, 125.4, 125.0, 115.8 (d, *J* = 21.3 Hz), 114.8 (d, *J* = 21.3 Hz) (not all carbon signals are resolved); ¹⁹F NMR (379 MHz) δ -115.43– -115.60 (m) -116.84 (ddd, *J* = 14.3, 8.8, 5.6 Hz); IR (Thin Film) ν 3073, 1602, 1509, 1461, 1389 cm⁻¹; HRMS (GC-QTOF) *m/z*: [M]⁺ Calcd for C₃₀H₁₇ClF₂ 450.0987, found 450.0972.

10-Chloro-2-fluoro-9-(4-fluorophenyl)indeno[1,2,3-*fg*]tetracene (7c):

Compound **6c** (1.425 g, 3.165 mmol) was dissolved in chloroform (20 mL) and the solution was purged with nitrogen for 3 minutes. Methanesulfonic acid was then added (80 mL) and the solution was purged with nitrogen for 5 minutes. 2,3-Dichloro-5,6-dicyano-1,4-benzoquinone (DDQ) (0.862 g, 3.798 mmol) was added to the mixture of chloroform and methanesulfonic acid and the solution was again purged with nitrogen for an additional 5 minutes. The reaction was stirred under nitrogen atmosphere for 3h, wrapped in aluminum foil to shield the mixture from light. The reaction progress was monitored using ¹H NMR and TLC, looking for the disappearance of fluorescence of the **6c** spot. The reaction was quenched by adding saturated NaHCO₃ solution (approximately 100 mL, CAUTION: Gas evolution, exothermic) to the reaction followed by pouring the reaction mixture into a separatory funnel containing solid NaHCO₃ (at least 10g CAUTION: Gas evolution, exothermic). After allowing to cool to room temperature, the mixture was extracted with chloroform (3 × 200 mL) and the remaining solid

1
2
3 NaHCO₃ was dissolved in water. The chloroform washes were combined and washed repeatedly
4
5 with saturated NaHCO₃ solution until the aqueous portion is clear and nearly colorless (faint
6
7 yellow, usually five washes). Then the organic portion was washed repeatedly with water until
8
9 the aqueous layer was no longer yellow. The organic layer was then washed with brine, dried
10
11 over magnesium sulfate, concentrated and placed under high vacuum overnight. The crude
12
13 product **7c** was dissolved in boiling chloroform followed by the addition of room temperature
14
15 methanol and the mixture was placed in the refrigerator (5 °C) overnight. Compound **7c** was
16
17 collected by vacuum filtration as a purple solid (1.150 g, 2.561, 81%): mp 295–296 °C; ¹H NMR
18
19 (400 MHz CDCl₃) δ 8.81 (d, *J* = 8.9 Hz, 1H), 8.60 (d, *J* = 9.2 Hz, 1H), 8.46 (dd, *J* = 8.6, 5.3 Hz,
20
21 1H), 8.18 (dd, *J* = 9.9, 2.3 Hz, 1H), 7.77–7.64 (m, 2H), 7.66–7.61 (m, 1H), 7.59–7.52 (m, 1H),
22
23 7.44–7.33 (m, 3H), 7.30–7.27 (m, 2H), 7.25–7.15 (m, 1H); ¹⁹F NMR (379 MHz, CDCl₃) δ -
24
25 115.68 (td, *J* = 9.3, 5.2 Hz), -115.94 – -116.09 (m); IR (Thin Film) ν 2917, 1602, 1507, 1460,
26
27 1395 cm⁻¹; HRMS (GC-QTOF) *m/z*: [M]⁺ Calcd for C₃₀H₁₅ClF₂ 448.0830; found 448.0813. A
28
29 suitable ¹³C NMR spectrum could not be obtained due to poor solubility.
30
31
32
33

34 35 **2-Fluoro-9-(4-fluorophenyl)-10-phenylindeno[1,2,3-*fg*]tetracene (8c):**

36
37 In a flame dried 250 mL 2-neck round bottom flask, anhydrous THF (150 mL), compound **7c**
38
39 (1.0981 g, 2.451 mmol), and PEPPSI-IPR™ (0.067 g, 0.09 mmol) were added and the solution
40
41 was purged with nitrogen for 10 minutes. The reaction was heated to 65 °C, at which point
42
43 phenyl magnesium bromide was added (1 M in THF, 3.677 mL, 0.667 g, 3.677 mmol). The
44
45 solution was maintained at 65 °C under a nitrogen atmosphere and wrapped in aluminum foil
46
47 overnight. The reaction was monitored by ¹H NMR. Upon complete consumption of **7c**, the
48
49 reaction was allowed to cool to room temperature and quenched with water (2 mL). THF was
50
51 removed in vacuo, then the resulting solid was dissolved in chloroform (600 mL). The organic
52
53
54
55
56
57
58
59
60

1
2
3 extract was washed once with saturated NaHCO₃ solution, once with water, once with brine,
4
5 dried over MgSO₄, concentrated, and placed under high vacuum overnight. Crude compound **8c**
6
7 was dissolved in boiling chloroform followed by the addition of room temperature methanol and
8
9 placed in the refrigerator (5 °C) overnight. Compound **8c** was collected by vacuum filtration as a
10
11 purple solid (1.076 g, 2.193 mmol, 90%): phase change 265 °C, sublimes 278 °C; ¹H NMR (500
12
13 MHz CDCl₃) δ 8.87 (d, *J* = 8.9 Hz, 1H), 8.82 (d, *J* = 8.9 Hz, 1H), 8.54 (dd, *J* = 8.5, 5.3 Hz, 1H),
14
15 8.29 (dd, *J* = 9.9, 2.4 Hz, 1H), 7.71–7.58 (m, 2H), 7.48–7.34 (m, 2H), 7.28–7.20 (m, 4H), 7.17–
16
17 7.08 (m, 2H), 6.97–6.93 (m, 2H), 6.93–6.84 (m, 2H), 6.85–6.67 (m, 1H); ¹³C NMR (125 MHz
18
19 CDCl₃) δ 133.2, 133.1, 131.6, 129.4, 129.2, 129.0, 128.0, 127.7, 127.4, 126.5, 124.9, 124.8,
20
21 124.7 (d, *J* = 6.8 Hz), 123.3, 114.23 (d, *J* = 21.4 Hz), 113.1 (d, *J* = 22.8 Hz), 111.8 (d, *J* = 24.9
22
23 Hz) (not all carbon signals are resolved); ¹⁹F NMR (379 MHz, CDCl₃) δ -116.27 (td, *J* = 9.3, 5.2
24
25 Hz), -117.61 – -117.81 (m); IR (Thin Film) ν 2957, 2916, 2849, 1601, 1508, 1469, 1460 cm⁻¹;
26
27 HRMS (GC-QTOF) *m/z*: [M]⁺ Calcd for C₃₆H₂₀F₂ 490.1533; found 490.1526.
28
29
30
31
32

33 **6-Chloro-5,12-bis(4-(trifluoromethyl)phenyl)-5,12-dihydrotetracene-5,12-diol (5d):**

34
35 6-chloro-5,12-bis(4-(trifluoromethyl)phenyl)-5,12-dihydrotetracene-5,12-diol was synthesized
36
37 analogously to 6-chloro-5,12-bis(4-fluorophenyl)-5,12-dihydrotetracene-5,12-diol, compound
38
39 **5c**. The product was carried to the next step without purification.
40
41

42 **5-Chloro-6,11-bis(4-(trifluoromethyl)phenyl)tetracene (6d):**

43
44 5-chloro-6,11-bis(4-(trifluoromethyl)phenyl)tetracene (**6d**) was synthesized analogously to 5-
45
46 chloro-6,11-bis(4-fluorophenyl)tetracene, compound **6c**, to give an orange/red solid (2 steps,
47
48 2.309 g, 4.191 mmol, 46%): mp 249-250 °C; ¹H NMR (500 MHz CDCl₃) δ 8.38 (dd, *J* = 8.3, 1
49
50 Hz, 1H), 8.21 (s, 1H), 7.96 (d, *J* = 7.9 Hz, 1H), 7.82 (d, *J* = 7.9 Hz, 1H), 7.79 (d, *J* = 8.7 Hz,
51
52 1H), 7.66 (d, *J* = 7.8 Hz, 2H), 7.61 (d, *J* = 7.8 Hz, 2H), 7.57–7.45 (m, 3H), 7.38 (dd, *J* = 8.7, 6.1
53
54
55
56
57
58
59
60

1
2
3 Hz, 1H), 7.30 (dd, $J = 7.1, 3.2$ Hz, 2H); ^{13}C NMR (125 MHz CDCl_3) δ 146.0, 143.1, 136.9,
4
5 134.9, 131.8, 131.7, 131.5, 130.9, 130.4, 130.3 (q, 36 Hz) 129.6, 129.5 (q, 36 Hz), 129.0, 128.7,
6
7 128.6, 127.6, 127.0, 126.3, 126.1, 126.1, 125.2, 124.9, 125.7 (q, 4 Hz), 124.7 (q, 4 Hz) 124.5 (q,
8
9 270 Hz) 124.3 (q, 270 Hz) (not all carbon signals are resolved); ^{19}F NMR (379 MHz, CDCl_3) δ -
10
11 63.36, -63.62; IR (Thin Film) ν 3074, 1616, 1461, 1406, 1324 cm^{-1} ; HRMS (GC-QTOF) m/z :
12
13 $[\text{M}]^+$ Calcd for $\text{C}_{32}\text{H}_{17}\text{ClF}_6$ 550.0923; found 550.0941.

14
15
16
17 **10-Chloro-2-(trifluoromethyl)-9-(4-(trifluoromethyl)phenyl)indeno[1,2,3-*fg*]tetracene (7d):**

18
19 10-chloro-2-(trifluoromethyl)-9-(4-(trifluoromethyl)phenyl)indeno[1,2,3-*fg*]tetracene was
20
21 synthesized analogously to 10-chloro-2-fluoro-9-(4-fluorophenyl)indeno[1,2,3-*fg*]tetracene,
22
23 compound **7c**, to give a purple/black solid (0.8479 g, 1.545 mmol, 40%): mp 259–260 °C; ^1H
24
25 NMR (400 MHz CDCl_3) δ 8.89 (d, $J = 8.9$ Hz, 1H), 8.84 (d, $J = 8.8$ Hz, 1H), 8.71 (s, 1H), 8.64
26
27 (d, $J = 8.2$ Hz, 1H), 8.58 (d, $J = 9.1$ Hz, 1H), 7.87–7.81 (m, 2H), 7.82–7.68 (m, 3H), 7.64–7.55
28
29 (m, 4H), 7.41 (dd, $J = 10.1, 6.4$ Hz, 1H); ^{19}F NMR (379 MHz, CDCl_3) δ -63.05, -63.45; IR (Thin
30
31 Film) ν 3071, 1679, 1617, 1595, 1432, 1405, 1324 cm^{-1} ; HRMS (GC-QTOF) m/z : $[\text{M}]^+$ Calcd
32
33 for $\text{C}_{32}\text{H}_{15}\text{ClF}_6$ 548.0766; found 548.0774. A suitable ^{13}C NMR spectrum could not be obtained
34
35 due to poor solubility.

36
37
38
39
40 **10-Phenyl-2-(trifluoromethyl)-9-(4-(trifluoromethyl)phenyl)indeno[1,2,3-*fg*]tetracene (8d):**

41
42 In a flame dried 250 mL 3-neck round bottom flask, anhydrous toluene (150 mL), compound **7d**
43
44 (0.8038 g, 1.467 mmol), and PEPSI-IPRTM (0.040 g, 0.05868 mmol) were added and the
45
46 solution was purged with nitrogen for 10 minutes. The reaction was heated to 65 °C at which point
47
48 phenylmagnesium bromide was added (1 M in THF, 2.200 mL, 2.200 mmol). The solution was
49
50 maintained at 65 °C under a nitrogen atmosphere wrapped in aluminum foil overnight. The
51
52 reaction was monitored by ^1H NMR. Upon complete consumption of **7d**, the reaction was
53
54
55
56
57
58
59
60

1
2
3 allowed to cool to room temperature and quenched with water (2 mL). Toluene was removed in
4 vacuo and the resulting solid was dissolved in chloroform (600 mL). The chloroform solution
5
6 was washed once with saturated NaHCO₃ solution, once with water, once with brine, dried over
7
8 MgSO₄, concentrated, and placed under high vacuum overnight. The crude product was
9
10 dissolved in boiling chloroform followed by the addition of room temperature methanol and
11
12 placed in the refrigerator (5 °C) overnight. Compound **8d** was collected by vacuum filtration, a
13
14 purple/black solid (0.7947 g, 1.346 mmol, 92%): mp 228–229 °C; ¹H NMR (400 MHz CDCl₃) δ
15
16 8.94 (d, *J* = 9.0 Hz, 1H), 8.90 (d, *J* = 8.9 Hz, 1H), 8.82 (s, 1H), 8.71 (d, *J* = 8.2 Hz, 1H), 7.82 (d,
17
18 *J* = 8.1 Hz, 1H), 7.73–7.64 (m, 2H), 7.41 (d, *J* = 9.0 Hz, 1H), 7.37–7.25 (m, 5H), 7.22–7.14 (m,
19
20 *J* = 8.1 Hz, 1H), 7.14–6.96 (m, 4H), 6.92 (dd, *J* = 8.1, 1.3 Hz, 1H); ¹³C NMR (125 MHz CDCl₃) δ 143.9,
21
22 142.2, 141.6, 140.3, 134.2, 133.6, 131.8, 131.6, 130.2, 129.6, 129.5, 129.5, 129.4, 128.9, 128.8,
23
24 128.7, 128.5, 128.4, 128.4, 127.5, 127.0, 125.2, 125.4, 124.2 (q, *J* = 3.7 Hz), 124.0, 123.7, 123.5,
25
26 120.6, 120.6 (not all carbon signals are resolved); ¹⁹F NMR (379 MHz, CDCl₃) δ -62.92, -64.91;
27
28 IR (Thin Film) ν 3060, 2351, 1615, 1551, 1448, 1364, 1324 cm⁻¹; HRMS (GC-QTOF) *m/z*: [M]⁺
29
30 Calcd for C₃₈H₂₀F₆ 590.1469; found 590.1450. Due to poor solubility, not all expected ¹³C NMR
31
32 signals were observed.

40 **6-Chloro-5,12-bis(4-methoxyphenyl)-5,12-dihydrotetracene-5,12-diol (5e):**

41
42 6-chloro-5,12-bis(4-methoxyphenyl)-5,12-dihydrotetracene-5,12-diol was synthesized
43
44 analogously to 6-chloro-5,12-bis(4-fluorophenyl)-5,12-dihydrotetracene-5,12-diol, compound
45
46 **5c**. The product was carried to the next step without purification.

49 **5-Chloro-6,11-bis(4-methoxyphenyl)tetracene (6e):**

50
51 5-chloro-6,11-bis(4-methoxyphenyl)tetracene (**6e**) was synthesized analogously to 5-chloro-
52
53 6,11-bis(4-fluorophenyl)tetracene, compound **6c**, to give an orange/red solid (2 steps, 1.0323 g,
54
55
56
57
58
59
60

2.173 mmol, 55%): mp 205–206 °C; ^1H NMR (500 MHz CDCl_3) δ 8.40 (dd, $J = 8.3$, 1 Hz, 1H), 8.36 (s, 1H), 7.77 (d, $J = 8.7$ Hz, 1H), 7.74–7.67 (m, 1H), 7.68–7.62 (m, 1H), 7.49–7.40 (m, 3H), 7.39–7.30 (m, 3H), 7.29–7.23 (m, 2H), 7.23–7.14 (m, 2H), 7.15–7.06 (m, 2H), 4.01 (s, 2H), 3.98 (s, 3H); ^{13}C NMR (125 MHz CDCl_3) δ 159.2, 158.8, 137.8, 135.6, 134.2, 132.5, 132.4, 132.2, 131.3, 130.5, 130.4, 130.1, 129.5, 128.8, 128.6, 127.4, 126.9, 126.9, 126.5, 125.8, 125.3, 125.1, 125.0, 114.0, 113.1, 55.4, 55.3. (not all carbon signals are resolved); IR (Thin Film) ν 2953, 2834, 1607, 1511, 1460, 1388 cm^{-1} ; HRMS (GC-QTOF) m/z : $[\text{M}]^+$ Calcd for $\text{C}_{32}\text{H}_{23}\text{ClO}_2$ 474.1387; found 474.1382.

10-Chloro-2-methoxy-9-(4-methoxyphenyl)indeno[1,2,3-*fg*]tetracene (7e):

10-chloro-2-methoxy-9-(4-methoxyphenyl)indeno[1,2,3-*fg*]tetracene was synthesized analogously to 10-chloro-2-fluoro-9-(4-fluorophenyl)indeno[1,2,3-*fg*]tetracene, compound **7c**, to give an purple/black solid (0.341 g, 0.721 mmol, 69%): mp 260–264 °C; ^1H NMR (400 MHz CDCl_3) δ 8.83 (d, $J = 5.1$ Hz, 1H), 8.81 (d, $J = 5.2$ Hz, 1H), 8.63 (d, $J = 9.1$ Hz, 1H), 8.43 (d, $J = 8.5$ Hz, 1H), 8.08 (d, $J = 2.3$ Hz, 1H), 7.77 (d, $J = 9.1$ Hz, 1H), 7.67 (dd, $J = 9.3$, 5.9 Hz, 1H), 7.60 (dd, $J = 9.3$, 5.9 Hz, 1H), 7.55 (dd, $J = 8.7$, 6.9 Hz, 1H), 7.41–7.30 (m, 3H), 7.18–7.09 (m, 2H), 7.05 (dd, $J = 8.5$, 2.3 Hz, 1H), 4.07 (s, 3H), 4.01 (s, 3H); IR (Thin Film) ν 3058, 2934, 2832, 1606, 1576, 1510, 1460, 1431, 1397 cm^{-1} ; HRMS (GC-QTOF) m/z : $[\text{M}]^+$ Calcd for $\text{C}_{32}\text{H}_{21}\text{ClO}_2$ 472.1230, found 472.1237. Due to poor solubility, a ^{13}C NMR spectrum could not be obtained.

2-Methoxy-9-(4-methoxyphenyl)-10-phenylindeno[1,2,3-*fg*]tetracene (8e):

2-methoxy-9-(4-methoxyphenyl)-10-phenylindeno[1,2,3-*fg*]tetracene, compound **8e**, was synthesized analogously to 2-fluoro-9-(4-fluorophenyl)-10-phenylindeno[1,2,3-*fg*]tetracene, compound **8c**, to give a purple solid (0.2020 g, 0.393 mmol, 54%): mp 212–213 °C; ^1H NMR

(400 MHz CDCl₃) δ 8.85 (d, *J* = 8.9 Hz, 1H), 8.83 (d, *J* = 8.9 Hz, 1H), 8.47 (d, *J* = 8.5 Hz, 1H), 8.15 (d, *J* = 2.3 Hz, 1H), 7.58 (ddd, *J* = 8.8, 6.4, 1.0 Hz, 2H), 7.55 (ddd, *J* = 8.8, 6.4, 1.0 Hz, 2H), 7.44 (d, *J* = 9.1 Hz, 1H), 7.36 (d, *J* = 9.1 Hz, 1H), 7.23–7.17 (m, 2H), 7.14–7.04 (m, 4H), 6.93 (dd, *J* = 8.0, 1.2 Hz, 2H), 6.57 (dd, *J* = 8.6, 2 Hz, 1H), 4.07 (s, 3H), 3.84 (s, 3H); ¹³C NMR (125 MHz CDCl₃) δ 159.1, 157.8, 141.5, 141.2, 140.6, 139.2, 134.4, 133.9, 133.0, 132.7, 132.5, 131.6, 131.1, 130.8, 129.3, 129.3, 128.8, 128.1, 127.4, 127.2, 127.1, 126.0, 124.7, 124.7, 124.4, 124.3, 123.8, 123.5, 113.0, 111.7, 110.9, 55.8, 55.3. (not all carbon signals are resolved); IR (Thin Film) ν 3000, 2954, 2834, 1675, 1607, 1573, 1511, 1461, 1441, 1411, 1389, 1360, 1315 cm⁻¹; HRMS (GC-QTOF) *m/z*: [M]⁺ Calcd for C₃₈H₂₆O₂ 514.1933; found 514.1926.

6-Chloro-5,12-bis(4-ethylphenyl)-5,12-dihydrotetracene-5,12-diol (5f):

6-chloro-5,12-bis(4-ethylphenyl)-5,12-dihydrotetracene-5,12-diol was synthesized analogously to 6-chloro-5,12-diphenyl-5,12-dihydrotetracene-5,12-diol, compound **5a**. The crude product was carried to the next step without purification.

5-Chloro-6,11-bis(4-ethylphenyl)tetracene (6f):

5-chloro-6,11-bis(4-ethylphenyl)tetracene was synthesized analogously to 5-chloro-6,11-diphenyltetracene, compound **6a**, to give an red/orange solid (0.343 g, 0.730 mmol, 73% yield over 2 steps): mp 160–161 °C; ¹H NMR (CDCl₃, 500 MHz) δ 8.39 (d, *J* = 9.1 Hz, 1H), 8.36 (s, 1H), 7.77 (d, *J* = 8.5 Hz, 1H), 7.68 (dt, *J* = 7.3, 2.5 Hz, 1H), 7.63 (dt, *J* = 6.0, 2.4 Hz, 1H), 7.51–7.47 (m, 2H), 7.46–7.39 (m, 3H), 7.32 (dd, *J* = 8.3, 6.6 Hz, 1H), 7.28–7.22 (m, 2H), 2.96–2.82 (m, 4H), 1.48–1.38 (m, 6H); ¹H NMR (400 MHz, CD₂Cl₂) δ 8.37–8.35 (m, 2H), 7.76 (d, *J* = 8.4 Hz, 1H), 7.65–7.62 (m, 1H), 7.61–7.59 (m, 1H), 7.51–7.49 (m, 2H), 7.46–7.44 (m, 1H), 7.42–7.40 (m, 2H), 7.39–7.35 (m, 4H), 7.33–7.31 (m, 1H), 7.24 (dt, *J* = 6.8, 2.9 Hz, 2H), 2.86 (dq, *J* = 15.1, 7.6 Hz, 4H), 1.41 (dt, *J* = 10.9, 7.6 Hz, 6H); ¹³C NMR (CDCl₃, 125 MHz) δ 143.6, 143.0,

1
2
3 139.2, 138.2, 136.4, 136.1, 132.0, 131.4, 130.5, 130.1, 129.4, 128.6, 128.0, 127.1, 126.9, 126.6,
4
5 125.7, 125.3, 125.0, 125.0, 125.0, 28.8, 15.7, 15.6 (not all carbon signals are resolved); IR (KBr)
6
7 ν 3022, 2964, 2930, 1511, 1460, 1389, 1360, 1316 cm^{-1} ; HRMS (ESI-TOF) m/z : $[\text{M}]^+$ Calcd for
8
9 $\text{C}_{34}\text{H}_{27}\text{Cl}$ 470.1801; found 470.1835.

10-Chloro-2-ethyl-9-(4-ethylphenyl)indeno[1,2,3-*fg*]tetracene (7f):

10-chloro-2-ethyl-9-(4-ethylphenyl)indeno[1,2,3-*fg*]tetracene was synthesized analogously to 10-
16 chloro-2-fluoro-9-(4-fluorophenyl)indeno[1,2,3-*fg*]tetracene, compound **7a**, to give an
17 purple/black solid (405 mg, 0.86 mmol, 67%): mp 246–250 °C; ^1H NMR (400 MHz, CDCl_3) δ
18 8.85 (d, $J = 8.8$ Hz, 1H), 8.85 (d, $J = 8.8$ Hz, 1H), 8.57 (d, $J = 9.1$ Hz, 1H), 8.40 (d, $J = 7.9$ Hz,
19 20 8.85 (d, $J = 8.8$ Hz, 1H), 8.57 (d, $J = 9.1$ Hz, 1H), 8.40 (d, $J = 7.9$ Hz,
21 22 1H), 8.30 (s, 1H), 7.73 (d, $J = 9.1$ Hz, 1H), 7.64 (dd, $J = 8.8, 6.5$ Hz, 1H), 7.58 (dd, $J = 8.8, 6.5$
23 24 1H), 8.30 (s, 1H), 7.73 (d, $J = 9.1$ Hz, 1H), 7.64 (dd, $J = 8.8, 6.5$ Hz, 1H), 7.58 (dd, $J = 8.8, 6.5$
25 26 Hz, 1H), 7.51 (dd, $J = 9.1, 6.4$ Hz, 1H), 7.41–7.37 (m, 2H), 7.35–7.28 (m, 4H), 2.97–2.79 (m,
27 28 4H), 1.49–1.37 (m, 6H); ^{13}C NMR (100 MHz, CDCl_3) δ 143.4, 143.3, 139.7, 138.5, 138.1, 137.3,
29 30 134.3, 131.8, 131.7, 131.7, 131.3, 131.0, 130.8, 129.4, 129.3, 129.1, 128.6, 127.7, 127.5, 127.4,
31 32 127.0, 126.6, 126.0, 124.9, 124.3, 124.1, 123.9, 123.0, 29.5, 28.8, 16.0, 15.7(not all carbon
33 34 signals are resolved); IR (Thin film) ν 3045, 2963, 2930, 2871, 1677, 1615, 1559, 1511, 1459,
35 36 1435, 1394, 1375, 1337, 1305 cm^{-1} ; HRMS (GC-QTOF) m/z : $[\text{M}]^+$ Calcd for $\text{C}_{34}\text{H}_{25}\text{Cl}$
37 38 468.1645; found 468.1664.

2-Ethyl-9-(4-ethylphenyl)-10-phenylindeno[1,2,3-*fg*]tetracene (8f):

Compound **8f** was synthesized analogously to 2-fluoro-9-(4-fluorophenyl)-10-
46 phenylindeno[1,2,3-*fg*]tetracene, compound **8c**, to give an purple/black solid to give an purple
47 solid (31 mg, 0.061 mmol, 74 %): mp 165–167 °C; ^1H NMR (400 MHz, CDCl_3) δ 8.94 (dd, 2H,
48 49 $J = 20.8, 8.8$ Hz), 8.52 (d, 1H, $J = 8.0$ Hz), 8.42 (s, 1H), 7.61–7.54 (m, 2H), 7.43–7.34 (m, 3H),
50 51 7.22–7.18 (m, 2H), 7.11–7.01 (m, 3H), 6.94–6.91 (m, 2H), 6.86–6.82 (m, 4H), 2.94 (q, $J = 7.6$
52 53 54 55 56 57 58 59 60

1
2
3 Hz, 2H), 2.62 (t, $J = 7.6$ Hz, 2H), 1.47 (t, $J = 7.6$ Hz, 3H) 1.31 (t, $J = 7.6$ Hz, 3H); IR (Thin Film)
4
5 ν 3054, 2961, 2927, 2869, 1602, 1553, 1511, 1458, 1440, 1397, 1362, 755, 737, 700 cm^{-1} ;
6
7
8 HRMS (GC-QTOF) m/z : $[M]^+$ Calcd for $\text{C}_{40}\text{H}_{30}$ 510.2348, found 510.2366. Due to poor
9
10 solubility, a ^{13}C NMR spectrum could not be obtained.
11
12

13 **6-Chloro-5,12-bis(4-propylphenyl)-5,12-dihydrotetracene-5,12-diol (5g):**

14
15 6-chloro-5,12-bis(4-propylphenyl)-5,12-dihydrotetracene-5,12-diol was synthesized analogously
16
17 to 6-chloro-5,12-diphenyl-5,12-dihydrotetracene-5,12-diol, compound **5a**. The crude product
18
19 was carried to the next step without purification.
20
21

22 **5-Chloro-6,11-bis(4-propylphenyl)tetracene (6g):**

23
24 5-chloro-6,11-bis(4-propylphenyl)tetracene was synthesized analogously to 5-chloro-6,11-
25
26 diphenyltetracene, compound **6a**, to give an red/orange solid (0.800 g, 1.50 mmol, 80% yield
27
28 over 2 steps): mp 167-168 $^{\circ}\text{C}$; ^1H NMR (CDCl_3 , 500 MHz) δ 8.39 (dd, $J = 8.2$ Hz, 1 Hz, 1H),
29
30 8.35 (s, 1H), 7.76 (d, $J = 8.7$ Hz, 1H), 7.72–7.65 (m, 1H), 7.65–7.59 (m, 1H), 7.50–7.44 (m, 3H),
31
32 7.43–7.39 (m, 2H), 7.39–7.34 (m, 3H), 7.34–7.28 (m, 2H), 7.26–7.23 (m, 2H), 2.91–2.70 (m,
33
34 4H), 1.93–1.76 (m, 4H), 1.15–1.04 (m, 6H) ; ^{13}C NMR (CDCl_3 , 125 MHz) δ 142.1, 141.3, 139.2,
35
36 138.1, 136.4, 136.0, 131.9, 131.2, 131.2, 130.5, 130.2, 130.0, 129.3, 128.8, 128.6, 127.7, 127.4,
37
38 126.8, 126.5, 125.6, 125.3, 125.0, 125.0, 124.9, 37.9, 37.9, 24.6, 24.5, 14.0, 13.8 (not all carbon
39
40 signals are resolved); IR (KBr) ν 3074, 3023, 2929, 2958, 2870, 1511, 1461, 1407, 1389, 1361,
41
42 1316 cm^{-1} ; HRMS (GC-QTOF) m/z : $[M]^+$ Calcd for $\text{C}_{36}\text{H}_{31}\text{Cl}$ 498.2114; found 498.2131.
43
44
45
46
47

48 **10-Chloro-2-propyl-9-(4-propylphenyl)indeno[1,2,3-*fg*]tetracene (7g):**

49
50 10-chloro-2-propyl-9-(4-propylphenyl)indeno[1,2,3-*fg*]tetracene (**7g**) was synthesized
51
52 analogously to 9-chloro-10-phenylindeno[1,2,3-*fg*]tetracene, compound **7a**, to give a
53
54 purple/black solid (14 mg, 0.032 mmol, 47%): mp 200–202 $^{\circ}\text{C}$; ^1H NMR (400 MHz, CDCl_3) δ
55
56
57
58
59
60

1
2
3 temperature and *p*-fluorophenylmagnesium bromide in THF (0.72 M, 10 mL, 7.27 mmol) was
4 added. The reaction was heated to 60 °C and stirred for 4 h. The reaction was then quenched
5 with 1N HCl and extracted with EtOAc (2 × 50 mL). The organic layers were combined, dried
6 over Na₂SO₄ and concentrated under vacuum. The residue was purified by flash column
7 chromatography (silica gel, 2% ethyl acetate in hexanes (R_f=0.30) to give impure compound **8h**
8 (222 mg, 0.470 mmol, 65%). In order to obtain pure product in a solid form, the product
9 obtained from chromatography was purified by recrystallization in DCM/MeOH to give
10 compound **8h**, a purple/black solid (176 mg, 0.372 mmol, 51%): mp 243–244 °C; ¹H NMR (300
11 MHz, CDCl₃) δ 8.92 (d, *J* = 8.9 Hz, 2H), 8.60 (dd, *J* = 5.6, 3.2 Hz, 2H), 7.65–7.57 (m, 2H), 7.53
12 (dd, *J* = 5.6, 3.1 Hz, 2H), 7.36 (d, *J* = 9.1 Hz, 2H), 7.24–7.15 (m, 3H), 7.10 (t, *J* = 7.3 Hz, 2H),
13 (dd, *J* = 5.6, 3.1 Hz, 2H), 7.36 (d, *J* = 9.1 Hz, 2H), 7.24–7.15 (m, 3H), 7.10 (t, *J* = 7.3 Hz, 2H),
14 6.96–6.79 (m, 4H), 6.72 (t, *J* = 8.8 Hz, 2H); ¹³C NMR (75 MHz, CDCl₃) δ 161.35 (d, *J* = 221
15 Hz), 140.5, 140.3, 139.7, 139.6, 139.4, 134.1, 133.2, 133.1, 131.6, 129.2, 128.9, 128.8, 127.5,
16 127.5, 127.3, 126.9, 126.8, 126.3, 124.6, 124.6, 124.3, 123.9, 123.8, 114.1 (d, *J* = 21.5 Hz) (Not
17 all carbon signals are resolved, including the expected 3 bond C–F coupling); ¹⁹F NMR (379
18 MHz, CDCl₃) δ -117.88 (tt, *J* = 9.3, 5.8 Hz); IR (KBr) ν 3035, 3033, 1597, 1556, 1503, 1396,
19 1212, 1133 cm⁻¹; HRMS (ESI-TOF) *m/z*: [M]⁺ Calcd for C₃₆H₂₁F 472.1627; found 472.1614.

20 **9-Phenyl-10-(*p*-tolyl)indeno[1,2,3-*fg*]tetracene (8i):**

21 To a flame-dried 100 mL round-bottom flask, **7b** (791 mg, 1.92 mmol), PEPPSI-IPr (65.0 mg,
22 0.0957 mmol) and 15 mL freshly distilled 1,4-dioxane were added. The flask was then sealed
23 with a septum and placed under a nitrogen atmosphere. The solution was stirred at room
24 temperature and *p*-methyl-phenylmagnesium bromide in THF (1.28 M, 15 mL, 19.2 mmol) was
25 added. The reaction was heated to 60 °C and stirred for 4 h. The reaction was then quenched
26 with 1N HCl and extracted with EtOAc (2 × 50 mL). The organic layers were combined, dried
27
28
29
30
31
32
33
34
35
36
37
38
39
40
41
42
43
44
45
46
47
48
49
50
51
52
53
54
55
56
57
58
59
60

1
2
3 over Na₂SO₄ and concentrated under vacuum. The residue was passed through a silica plug,
4
5 eluted with 5% ethyl acetate in hexanes, and concentrated under vacuum. The crude product was
6
7 further purified by recrystallization in hot xylenes/*i*PrOH to give compound **8i**, a purple/black
8
9 solid (598 mg, 1.28 mmol, 67%): mp 180–181 °C; ¹H NMR (300 MHz, CDCl₃) δ 8.92 (d, *J* = 8.8
10
11 Hz, 2H), 8.60 (dd, *J* = 5.7, 3.2 Hz, 2H), 7.63–7.55 (m, 2H), 7.52 (dd, *J* = 5.7, 3.1 Hz, 2H), 7.47
12
13 (d, *J* = 9.1 Hz, 1H), 7.36 (d, *J* = 9.1 Hz, 1H), 7.25–7.17 (m, 2H), 7.15–7.10 (m, 1H), 7.02 (t, *J* =
14
15 7.5 Hz, 2H), 6.92 – 6.87 (m, 2H), 6.84–6.75 (m, 4H), 2.32 (s, 3H); ¹³C NMR (75 MHz, CDCl₃) δ
16
17 141.1, 140.9, 140.4, 139.7, 139.6, 137.0, 135.6, 134.0, 134.0, 131.6, 131.4, 130.9, 130.8, 129.4,
18
19 129.3, 129.0, 128.9, 128.3, 127.9, 127.5, 127.4, 127.0, 126.7, 126.6, 125.5, 124.6, 124.3, 124.3,
20
21 124.2, 123.8, 21.2. (Not all carbon signals are resolved); IR (KBr) ν 3041, 3022, 2892, 2852,
22
23 1558, 1511, 1469, 1451, 1440, 1430, 1396, 1360, 1297, 1136, 1020, 968 cm⁻¹; HRMS (ESI-
24
25 TOF) *m/z*: [M]⁺ Calcd for C₃₇H₂₄ 468.1878; found 468.1907.

30
31 **9-(Naphthalen-1-yl)-10-phenylindeno[1,2,3-*fg*]tetracene (8j):**

32
33 To a flame-dried 100 mL round-bottom flask, **7a** (800 mg, 1.94 mmol), PEPPSI-IPr (65.0 mg,
34
35 0.0957 mmol) and 15 mL freshly distilled 1,4-dioxane were added. The flask was then sealed
36
37 with a septum and placed under a nitrogen atmosphere. The solution was stirred at room
38
39 temperature and α-naphthylmagnesium bromide in THF (1.29 M, 15 mL, 19.4 mmol) was
40
41 added. The reaction was heated to 60 °C and stirred for 4 h. The reaction was then quenched
42
43 with 1N HCl and extracted with EtOAc (2 × 50 mL). The organic layers were combined, dried
44
45 over Na₂SO₄ and concentrated under vacuum. The residue was passed through a silica plug,
46
47 eluted with 5% ethyl acetate in hexanes and concentrated under vacuum. The crude was further
48
49 purified by recrystallization in hot chloroform/MeOH to give compound **8j**, a purple/black solid
50
51 (438 mg, 0.868 mmol, 45%): mp 243–244 °C; ¹H NMR (300 MHz, CDCl₃) δ 8.95 (t, *J* = 9.2 Hz,
52
53
54
55
56
57
58
59
60

1
2
3 2H), 8.64 (dt, $J = 6.0, 3.1$ Hz, 2H), 7.71 (d, $J = 8.1$ Hz, 1H), 7.64–7.53 (m, 5H), 7.35 (dd, $J =$
4
5 10.9, 4.0 Hz, 1H), 7.29–7.20 (m, 3H), 7.19–7.06 (m, 4H), 6.99 (d, $J = 8.4$ Hz, 1H), 6.91 (d, $J =$
6
7 6.3 Hz, 2H), 6.79–6.71 (m, 1H), 6.32 (d, $J = 6.6$ Hz, 2H); ^{13}C NMR (75 MHz, CDCl_3) δ 141.0,
8
9 139.7, 138.8, 138.7, 137.9, 134.2, 134.1, 134.0, 133.1, 131.4, 131.2, 131.1, 130., 129.8, 129.3,
10
11 129.0, 128.4, 127.7, 127.7, 127.6, 127.5, 127.3, 126.9, 126.8, 126.2, 125.9, 125.6, 125.4, 125.3,
12
13 125.0, 124.9, 124.7, 124.4, 124.3, 124.3, 123.9, 123.7 (not all carbon signal were resolved); IR
14
15 (KBr) ν 3041, 1595, 1596, 1558, 1504, 1469, 1452, 1439, 1382, 1360, 1298, 1256, 1187, 1171,
16
17 1139, 1016, 965 cm^{-1} ; HRMS (ESI-TOF) m/z : $[\text{M}]^+$ Calcd for $\text{C}_{40}\text{H}_{24}$ 504.1878; found 504.1840.

22 ***N,N*-Dimethyl-4-(10-phenylindeno[1,2,3-*fg*]tetracen-9-yl)aniline (8k):**

23
24 To a flame-dried 100 mL round-bottom flask, **7a** (500 mg, 1.21 mmol), PEPPSI-IPr (41.0 mg,
25
26 0.0603 mmol) and 10 mL freshly distilled 1,4-dioxane were added. The flask was then sealed
27
28 with a septum and placed under a nitrogen atmosphere. The solution was stirred at room
29
30 temperature and *p*-*N,N*-dimethylaminophenylmagnesium bromide in THF (1.21 M, 10 mL, 12.1
31
32 mmol) was added. The reaction was heated to 60 °C and stirred for 4 h. The reaction was then
33
34 quenched with 1N HCl and extracted with EtOAc (2 × 50 mL). The combined organic layer was
35
36 then washed with saturated NaHCO_3 solution and brine, dried over Na_2SO_4 and concentrated
37
38 under vacuum. The crude was further purified by recrystallization in DCM/MeOH to give **8k**, a
39
40 purple/black solid (286 mg, 0.575 mmol, 47%): mp 238–241 °C; ^1H NMR (300 MHz, CDCl_3) δ
41
42 8.92 (dd, $J = 8.6, 3.3$ Hz, 2H), 8.60 (dd, $J = 5.6, 3.3$ Hz, 2H), 7.63–7.59 (m, 3H), 7.52 (dd, $J =$
43
44 5.7, 3.1 Hz, 2H), 7.37 (d, $J = 9.1$ Hz, 1H), 7.25–7.16 (m, 2H), 7.12–7.02 (m, 3H), 6.96–6.90 (m,
45
46 2H), 6.79–6.72 (m, 2H), 6.42 (d, $J = 8.7$ Hz, 2H), 2.97 (s, 3H); ^{13}C NMR (75 MHz, CDCl_3) δ
47
48 149.1, 142.0, 141.2, 140.7, 139.8, 139.6, 134.5, 133.9, 132.1, 131.5, 130.9, 130.4, 129.7, 129.4,
49
50 129.1, 128.9, 128.4, 127.5, 127.3, 127.1, 126.6, 126.5, 126.0, 124.9, 124.2, 124.1, 123.8, 123.7,
51
52
53
54
55
56
57
58
59
60

1
2
3 112.2, 40.9 (Not all carbon signals are resolved); IR (KBr) ν 3857, 3747, 3654, 3043, 2786,
4
5 1610, 1517, 1468, 1443, 1394, 1344, 1298, 1191, 1166 cm^{-1} ; HRMS (ESI-TOF) m/z : $[M]^+$ Calcd
6
7 for $\text{C}_{38}\text{H}_{27}\text{N}$ 497.2143; found 497.2135.
8
9

10 **9-(4-Methoxyphenyl)-10-phenylindeno[1,2,3-*fg*]tetracene (8l)**

11
12 To a flame-dried 100 mL round-bottom flask, **7a** (400 mg, 0.969 mmol), dehydrated *para*-
13
14 methoxyphenylboronic acid (468 mg, 1.16 mmol), PEPPSI-IPr (13.0 mg, 0.0191 mmol),
15
16 potassium carbonate (670 mg, 4.85 mmol) and 50 mL freshly distilled toluene were added under
17
18 nitrogen. The solution was then heated to 90 °C and stirred for 24 h . The mixture was then
19
20 passed through a Celite plug to remove insoluble solids, which was rinsed with ethyl acetate.
21
22 The organic extracts were concentrated under vacuum. The residue was passed through a silica
23
24 plug, eluted with 10% ethyl acetate in hexanes to remove a small amount of unconsumed starting
25
26 material. The crude product was further purified by recrystallization in DCM/MeOH to give **8l**, a
27
28 purple/black solid (414 mg combined from two crops of crystals, 0.854 mmol, 88%): mp 158–
29
30 159 °C; ^1H NMR (300 MHz, CDCl_3) δ 8.92 (d, J = 8.9 Hz, 2H), 8.61 (dd, J = 5.7, 3.2 Hz, 2H),
31
32 7.59 (ddd, J = 8.9, 2.3, 1.2 Hz, 2H), 7.53 (dd, J = 5.7, 3.1 Hz, 2H), 7.47 (d, J = 9.2 Hz, 1H), 7.36
33
34 (d, J = 9.2 Hz, 1H), 7.24–7.18 (m, 2H), 7.15–7.05 (m, 3H), 6.96–6.91 (m, 2H), 6.83 (d, J = 8.7
35
36 Hz, 2H), 6.57 (d, J = 8.7 Hz, 2H), 3.84 (s, 3H); ^{13}C NMR (75 MHz, CDCl_3) δ 157.8, 140.9,
37
38 140.8, 140.5, 139.7, 139.7, 134.3, 134.0, 132.6, 132.4, 131.6, 131.0, 130.8, 129.4, 129.3, 129.0,
39
40 128.9, 128.3, 127.5, 127.4, 127.2, 126.7, 126.0, 124.7, 124.4, 124.2, 123.8, 112.9, 55.3 (Not all
41
42 carbon signals are resolved); IR (KBr) ν 3435, 3039, 2958, 2839, 1607, 1501, 1276, 1233, 1183,
43
44 1041, 1012 cm^{-1} ; HRMS (ESI-TOF) m/z : $[M]^+$ Calcd for $\text{C}_{37}\text{H}_{24}\text{O}$ 484.1827; found 484.1811.
45
46
47
48
49
50

51 ***N,N*-Dimethyl-4-(3-methyl-10-(*p*-tolyl)indeno[1,2,3-*fg*]tetracene-9-yl)aniline (8m):**

To a flame-dried 100 mL round-bottom flask, **7b** (400 mg, 0.998 mmol), PEPPSI-IPr (34.0 mg, 0.0500 mmol) and 10 mL freshly distilled 1,4-dioxane were added. The flask was then sealed with a septum and placed under a nitrogen atmosphere. The solution was stirred at room temperature and *p*-*N,N*-dimethylaminophenylmagnesium bromide in THF (1.00 M, 10 mL, 10.0 mmol) was added. The reaction was heated to 60 °C and stirred for 4 h. The reaction was then quenched with 1N HCl and extracted with EtOAc (2 × 50 mL). The combined organic layer was then washed with saturated NaHCO₃ solution and brine, dried over Na₂SO₄ and concentrated under vacuum. The crude was further purified by recrystallization in hot toluene/*i*PrOH (1:10) to give **8m**, a purple/black solid (353 mg, 0.672 mmol, 67%): mp 259–263 °C; ¹H NMR (300 MHz, CDCl₃) δ 8.92 (dd, *J* = 8.6, 3.3 Hz, 2H), 8.46 (d, *J* = 7.8 Hz, 1H), 8.40 (s, 1H), 7.58 (d, *J* = 9.4 Hz, 3H), 7.44 (d, *J* = 9.2 Hz, 1H), 7.32 (d, *J* = 7.8 Hz, 1H), 7.20 (dd, *J* = 15.6, 7.5 Hz, 2H), 6.86–6.77 (m, 4H), 6.76–6.68 (m, 2H), 6.40 (d, *J* = 8.5 Hz, 2H), 2.97 (s, 6H), 2.65 (s, 3H), 2.31 (s, 3H); IR (KBr) 3025, 2916, 2857, 2794, 1610, 1557, 1514, 1456, 1396, 1348, 1192, 1161 cm⁻¹; HRMS (ESI-TOF) *m/z*: [M]⁺ Calcd for C₄₀H₃₁N 525.2457; found 525.2431. Due to poor solubility, a ¹³C NMR spectrum could not be obtained.

10-(4-Fluorophenyl)-2-methyl-9-(*p*-tolyl)indeno[1,2,3-*fg*]tetracene (8n**):**

To a flame-dried 100 mL round-bottom flask, **7b** (400 mg, 0.907 mmol), PEPPSI-IPr (31.0 mg, 0.0456 mmol) and 10 mL freshly distilled 1,4-dioxane were added. The flask was then sealed with a septum and placed under a nitrogen atmosphere. The solution was stirred at room temperature and *p*-fluorophenylmagnesium bromide in THF (0.907 M, 10 mL, 9.07 mmol) was added. The reaction was heated to 60 °C and stirred for 4 h. The reaction was then quenched with 1N HCl and extracted with EtOAc (2 × 50 mL). The organic layers were combined, dried over Na₂SO₄ and concentrated under vacuum. The residue was purified by flash column

1
2
3 chromatography (silica gel, 5% ethyl acetate in hexanes, R_f 0.35) to give **8n** (278 mg, 0.555
4 mmol, 60%). In order to obtain the product in a solid form, the product obtained from
5 chromatography was purified by recrystallization in hot toluene/*i*PrOH (1:10) to give compound
6
7
8 **8n**, a purple/black solid (114 mg, 0.227 mmol, 25%): mp 231–232 °C; ^1H NMR (300 MHz,
9 CDCl_3) δ 8.89 (dd, $J = 17.7, 8.9$ Hz, 2H), 8.45 (d, $J = 7.9$ Hz, 1H), 8.40 (s, 1H), 7.58 (td, $J =$
10 15.8, 8.0 Hz, 2H), 7.44 (d, $J = 9.0$ Hz, 1H), 7.35 (t, $J = 8.3$ Hz, 2H), 7.20 (dd, $J = 9.1, 6.3$ Hz,
11 2H), 6.92–6.69 (m, 8H), 2.64 (s, 3H), 2.38 (s, 3H); ^{13}C NMR (75 MHz, CDCl_3) δ 140.0, 139.3,
12 137.3, 136.5, 135.9, 134.1, 134.0, 133.1, 133.0, 131.5, 129.3, 129.0, 128.7, 128.5, 128.0, 127.6,
13 127.3, 125.3, 124.8, 124.4, 123.93, 123.87, 114.1, 113.8 (d, $J = 21.5$ Hz), 22.1, 21.6 (Not all
14 carbon signals are resolved, the carbon *ipso* to the fluorine could not be extracted from noise);
15 ^{19}F NMR (379 MHz, CDCl_3) δ 118.23 (tt, $J = 9.1, 5.6$ Hz); IR (KBr) ν 3022, 2918, 2857, 1599,
16 1556, 1508, 1456, 1432, 1396, 1355, 1295, 1215, 1152, 1018 cm^{-1} ; HRMS (ESI-TOF) m/z : $[\text{M}]^+$
17 Calcd for $\text{C}_{38}\text{H}_{25}\text{F}$ 500.1940, found 500.1949.
18
19
20
21
22
23
24
25
26
27
28
29
30
31
32
33
34

35 ASSOCIATED CONTENT

36
37
38 **Supporting Information.** The following files are available free of charge: computational results,
39 crystallographic information files (CIF) for new crystal structures, copies of NMR spectra for
40 new compounds, X-Ray diffraction tabulated details.
41
42
43
44
45

46 AUTHOR INFORMATION

47 Corresponding Authors

48
49
50 Email: cramer@umn.edu, cdouglas@umn.edu

51
52
53
54
55
56
57
58
59
60
61
62
63
64
65
66
67
68
69
70
71
72
73
74
75
76
77
78
79
80
81
82
83
84
85
86
87
88
89
90
91
92
93
94
95
96
97
98
99
100
101
102
103
104
105
106
107
108
109
110
111
112
113
114
115
116
117
118
119
120
121
122
123
124
125
126
127
128
129
130
131
132
133
134
135
136
137
138
139
140
141
142
143
144
145
146
147
148
149
150
151
152
153
154
155
156
157
158
159
160
161
162
163
164
165
166
167
168
169
170
171
172
173
174
175
176
177
178
179
180
181
182
183
184
185
186
187
188
189
190
191
192
193
194
195
196
197
198
199
200
201
202
203
204
205
206
207
208
209
210
211
212
213
214
215
216
217
218
219
220
221
222
223
224
225
226
227
228
229
230
231
232
233
234
235
236
237
238
239
240
241
242
243
244
245
246
247
248
249
250
251
252
253
254
255
256
257
258
259
260
261
262
263
264
265
266
267
268
269
270
271
272
273
274
275
276
277
278
279
280
281
282
283
284
285
286
287
288
289
290
291
292
293
294
295
296
297
298
299
300
301
302
303
304
305
306
307
308
309
310
311
312
313
314
315
316
317
318
319
320
321
322
323
324
325
326
327
328
329
330
331
332
333
334
335
336
337
338
339
340
341
342
343
344
345
346
347
348
349
350
351
352
353
354
355
356
357
358
359
360
361
362
363
364
365
366
367
368
369
370
371
372
373
374
375
376
377
378
379
380
381
382
383
384
385
386
387
388
389
390
391
392
393
394
395
396
397
398
399
400
401
402
403
404
405
406
407
408
409
410
411
412
413
414
415
416
417
418
419
420
421
422
423
424
425
426
427
428
429
430
431
432
433
434
435
436
437
438
439
440
441
442
443
444
445
446
447
448
449
450
451
452
453
454
455
456
457
458
459
460
461
462
463
464
465
466
467
468
469
470
471
472
473
474
475
476
477
478
479
480
481
482
483
484
485
486
487
488
489
490
491
492
493
494
495
496
497
498
499
500
501
502
503
504
505
506
507
508
509
510
511
512
513
514
515
516
517
518
519
520
521
522
523
524
525
526
527
528
529
530
531
532
533
534
535
536
537
538
539
540
541
542
543
544
545
546
547
548
549
550
551
552
553
554
555
556
557
558
559
560
561
562
563
564
565
566
567
568
569
570
571
572
573
574
575
576
577
578
579
580
581
582
583
584
585
586
587
588
589
590
591
592
593
594
595
596
597
598
599
600
601
602
603
604
605
606
607
608
609
610
611
612
613
614
615
616
617
618
619
620
621
622
623
624
625
626
627
628
629
630
631
632
633
634
635
636
637
638
639
640
641
642
643
644
645
646
647
648
649
650
651
652
653
654
655
656
657
658
659
660
661
662
663
664
665
666
667
668
669
670
671
672
673
674
675
676
677
678
679
680
681
682
683
684
685
686
687
688
689
690
691
692
693
694
695
696
697
698
699
700
701
702
703
704
705
706
707
708
709
710
711
712
713
714
715
716
717
718
719
720
721
722
723
724
725
726
727
728
729
730
731
732
733
734
735
736
737
738
739
740
741
742
743
744
745
746
747
748
749
750
751
752
753
754
755
756
757
758
759
760
761
762
763
764
765
766
767
768
769
770
771
772
773
774
775
776
777
778
779
780
781
782
783
784
785
786
787
788
789
790
791
792
793
794
795
796
797
798
799
800
801
802
803
804
805
806
807
808
809
810
811
812
813
814
815
816
817
818
819
820
821
822
823
824
825
826
827
828
829
830
831
832
833
834
835
836
837
838
839
840
841
842
843
844
845
846
847
848
849
850
851
852
853
854
855
856
857
858
859
860
861
862
863
864
865
866
867
868
869
870
871
872
873
874
875
876
877
878
879
880
881
882
883
884
885
886
887
888
889
890
891
892
893
894
895
896
897
898
899
900
901
902
903
904
905
906
907
908
909
910
911
912
913
914
915
916
917
918
919
920
921
922
923
924
925
926
927
928
929
930
931
932
933
934
935
936
937
938
939
940
941
942
943
944
945
946
947
948
949
950
951
952
953
954
955
956
957
958
959
960
961
962
963
964
965
966
967
968
969
970
971
972
973
974
975
976
977
978
979
980
981
982
983
984
985
986
987
988
989
990
991
992
993
994
995
996
997
998
999
1000

Present Addresses

† Chemical & Analytical Development, Suzhou Novartis Pharma Technology Co., Ltd, #18
Tonglian Road, Riverside Industrial Park, Changshu Economic Development Zone, Changshu /
Jiangsu Province, 215537, China

Author Contributions

The manuscript was written through contributions of all authors. All authors have given approval to the final version of the manuscript.

Funding Sources

This work was supported in part by the U.S. Department of Energy, Office of Science, Office of Basic Energy Sciences, Division of Chemical Sciences, Geosciences, and Biosciences, the Office of Science, Office of Workforce Development for Teachers and Scientists, Office of Science Graduate Student Research (SCGSR) program, and the Office of Advanced Scientific Computing Research through the Scientific Discovery through Advanced Computing (SciDAC) program under Award Number DE-SC0008666. The SCGSR program is administered by the Oak Ridge Institute for Science and Education for the DOE under contract number DE-SC0014664. The National Science Foundation is acknowledged for support via the MRSEC program (DMR-1006566) and for a grant to purchase the Bruker-AXS D8 Venture single crystal diffractometer (MRI-1229400), along with the University of Minnesota.

ACKNOWLEDGMENT

The authors acknowledge the Minnesota Supercomputing Institute (MSI) at the University of Minnesota for providing resources that contributed to the research results reported within this

1
2
3 paper and Professor Laura Gagliardi for helpful discussions. CJD thanks DuPont for a Young
4
5 Professor Award.
6
7

8
9 REFERENCES

- 10
11
12 (1) Zhou, Y.; Ding, L.; Shi, K.; Dai, Y. Z.; Ai, N.; Wang, J.; Pei, J. *Adv. Mater.* **2012**, *24*,
13 957.
14 (2) Zhang, J.; Li, C. Z.; Williams, S. T.; Liu, S.; Zhao, T.; Jen, A. K. *J. Am. Chem. Soc.*
15 **2015**, *137*, 2167.
16 (3) Kim, Y.; Park, G.; Choi, S.; Lee, D.; Cho, M.; Choi, D. *J. Mater. Chem. C* **2017**, *5*, 7182.
17 (4) Hwang, Y. J.; Li, H.; Courtright, B. A.; Subramaniyan, S.; Jenekhe, S. A. *Adv. Mater.*
18 **2016**, *28*, 124.
19 (5) Meng, D.; Sun, D.; Zhong, C.; Liu, T.; Fan, B.; Huo, L.; Li, Y.; Jiang, W.; Choi, H.; Kim,
20 T.; Kim, J. Y.; Sun, Y.; Wang, Z.; Heeger, A. J. *J. Am. Chem. Soc.* **2016**, *138*, 375.
21 (6) Hendsbee, A. D.; Sun, J. P.; Rutledge, L. R.; Hill, I. G.; Welch, G. C. *J. Mater. Chem. A*
22 **2014**, *2*, 4198.
23 (7) Jones, B. A.; Ahrens, M. J.; Yoon, M. H.; Facchetti, A.; Marks, T. J.; Wasielewski, M. R.
24 *Angew. Chem., Int. Ed.* **2004**, *43*, 6363.
25 (8) Chase, D. T.; Fix, A. G.; Rose, B. D.; Weber, C. D.; Nobusue, S.; Stockwell, C. E.;
26 Zakharov, L. N.; Lonergan, M. C.; Haley, M. M. *Angew. Chem., Int. Ed.* **2011**, *50*, 11103.
27 (9) Buchholtz, F.; Zelichenok, A.; Krongauz, V. *Macromolecules* **1993**, *26*, 906.
28 (10) Li, M. M.; Liu, Y. T.; Ni, W.; Liu, F.; Feng, H. R.; Zhang, Y. M.; Liu, T. T.; Zhang, H.
29 T.; Wan, X. J.; Kan, B.; Zhang, Q.; Russell, T. P.; Chen, Y. S. *J. Mater. Chem. A* **2016**, *4*, 10409.
30 (11) Rananaware, A.; Gupta, A.; Kadam, G.; Duc La, D.; Bilic, A.; Xiang, W.; Evans, R., A.;
31 Bhosale, S., V. *Mater. Chem. Front.* **2017**, *1*, 2511.
32 (12) Gupta, A.; Rananaware, A.; Srinivasa Rao, P.; Duc La, D.; Bilic, A.; Xiang, W.; Li, J.;
33 Evans, R., A.; Bhosale, S., V.; Bhosale, S., V. *Mater. Chem. Front.* **2017**, *1*, 1600.
34 (13) Liu, F.; Zhou, Z.; Zhang, C.; Vergote, T.; Fan, H.; Liu, F.; Zhu, X. *J. Am. Chem. Soc.*
35 **2016**, *138*, 15523.
36 (14) Eftaiha, A. F.; Sun, J. P.; Hill, I. G.; Welch, G. C. *J. Mater. Chem. A* **2014**, *2*, 1201.
37 (15) Kondratenko, M.; Moiseev, A. G.; Perepichka, D. F. *J. Mater. Chem.* **2011**, *21*, 1470.
38 (16) Li, S. X.; Yan, J. L.; Li, C. Z.; Liu, F.; Shi, M. M.; Chen, H. Z.; Russell, T. P. *J. Mater.*
39 *Chem. A* **2016**, *4*, 3777.
40 (17) Shen, Z.; Xu, B.; Liu, P.; Hu, Y.; Yu, Y.; Ding, H.; Kloo, L.; Hua, J.; Sun, L.; Tian, H. *J.*
41 *Mater. Chem. A* **2017**, *5*, 1242.
42 (18) Jiang, H.; Ferrara, G.; Zhang, X.; Oniwa, K.; Islam, A.; Han, L.; Sun, Y. J.; Bao, M.;
43 Asao, N.; Yamamoto, Y.; Jin, T. *Chemistry* **2015**, *21*, 4065.
44 (19) Deng, Y.; Xu, B.; Castro, E.; Fernandez-Delgado, O.; Echevoyen, L.; Baldrige, K., K.;
45 Siegel, J., S. *Euro. J. Org. Chem.* **2017**, *2017*, 4338.
46 (20) Lee, C. H.; Plunkett, K. N. *Org. Lett.* **2013**, *15*, 1202.
47 (21) Zhu, X. J.; Bheemireddy, S. R.; Sambasivarao, S. V.; Rose, P. W.; Guzman, R. T.;
48 Walther, A. G.; DuBay, K. H.; Plunkett, K. N. *Macromolecules* **2016**, *49*, 127.
49 (22) Lu, R. Q.; Zheng, Y. Q.; Zhou, Y. N.; Yan, X. Y.; Lei, T.; Shi, K.; Zhou, Y.; Pei, J.;
50 Zoppi, L.; Baldrige, K. K.; Siegel, J. S.; Cao, X. Y. *J. Mater. Chem. A* **2014**, *2*, 20515.
51 (23) Gu, X.; Luhman, W. A.; Yagodkin, E.; Holmes, R. J.; Douglas, C. J. *Org. Lett.* **2012**, *14*,
52 1390.
53
54
55
56
57
58
59
60

- (24) We are currently analyzing unpublished data that demonstrate asymmetric indenotetracenes potential as an electron transport material in organic photovoltaics.
- (25) To remove inorganic tin from the product, the reaction mixture is made basic, filtered over diatomaceous earth, and further purified via trituration from hot chloroform with methonal..
- (26) Miao, Q.; Chi, X.; Xiao, S.; Zeis, R.; Lefenfeld, M.; Siegrist, T.; Steigerwald, M. L.; Nuckolls, C. *J. Am. Chem. Soc.* **2006**, *128*, 1340.
- (27) Zhai, L.; Shukla, R.; Wadumethrige, S. H.; Rathore, R. *J. Org. Chem.* **2010**, *75*, 4748.
- (28) Grzybowski, M.; Skonieczny, K.; Butenschon, H.; Gryko, D. T. *Angew. Chem. Int. Ed.* **2013**, *52*, 9900.
- (29) Smet, M.; Van Dijk, J.; Dehaen, W. *Synlett* **1999**, *4*, 495.
- (30) Eversloh, C., L.; Avlasevich, Y.; Li, C.; Mullen, K. *Chemistry* **2011**, *17*, 12756.
- (31) Lakshminarayana, A., N.; Chang, J.; Luo, J.; Zheng, B.; Huang, K. W.; Chi, C. *Chem. Commun.* **2015**, *51*, 3604.
- (32) Wu, J.; Pisula, W.; Mullen, K. *Chem. Rev.* **2007**, *107*, 718.
- (33) Avlasevich, Y.; Kohl, C.; Mullen, K. *J. Mater. Chem.* **2006**, *16*, 1053.
- (34) Zhai, L.; Shukla, R.; Rathore, R. *Org. Lett.* **2009**, *11*, 3474.
- (35) Yagodkin, E.; Douglas, C. J. *Tetrahedron Lett* **2010**, *51*, 3037.
- (36) O'Brien, C. J.; Kantchev, E. A.; Valente, C.; Hadei, N.; Chass, G. A.; Lough, A.; Hopkinson, A. C.; Organ, M. G. *Chem. Eur. J.* **2006**, *12*, 4743.
- (37) Compounds **8a-i** were chraterized by ^1H , ^{13}C , ^{19}F NMR and IR. HRMS was done via QTOF and ESI. Single-crystal X-ray structures were obtain for compounds **8a-e, h**.
- (38) Dexter, D. L. *J. Chem. Phys* **1953**, *21*, 836.
- (39) CIFs found in the supporting information
- (40) The degree of indenotetracene core overlap and pi-stacking distance were measured from the solved crystal structures.
- (41) Coropceanu, V.; Cornil, J.; da Silva Filho, D. A.; Olivier, Y.; Silbey, R.; Bredas, J. L. *Chem. Rev.* **2007**, *107*, 926.
- (42) Sonar, P.; Williams, E. L.; Singh, S. P.; Manzhos, S.; Dodabalapur, A. *Phys. Chem. Chem. Phys.* **2013**, *15*, 17064.
- (43) Lan, L. Y.; Chen, Z. M.; Ying, L.; Huang, F.; Cao, Y. *Org Electron* **2016**, *30*, 176.
- (44) Valenti, G.; Bruno, C.; Rapino, S.; Fiorani, A.; Jackson, E. A.; Scott, L. T.; Paolucci, F.; Marcaccio, M. *J. Phys. Chem. C* **2010**, *114*, 19467.
- (45) Zhu, X. J.; Yuan, B. X.; Plunkett, K. N. *Tetrahedron Lett* **2015**, *56*, 7105.
- (46) Bheemireddy, S. R.; Ubaldo, P. C.; Rose, P. W.; Finke, A. D.; Zhuang, J.; Wang, L.; Plunkett, K. N. *Angew. Chem., Int. Ed.* **2015**, *54*, 15762.
- (47) Zhou, K.; Dong, H.; Zhang, H. L.; Hu, W. *Phys. Chem. Chem. Phys.* **2014**, *16*, 22448.
- (48) Li, H. Y.; Earmme, T.; Subramaniyan, S.; Jenekhe, S. A. *Adv. Energy Mater.* **2015**, *5*, 1402041.
- (49) Zhou, F.; Jehoulet, C.; Bard, A. J. *J. Am. Chem. Soc.* **1992**, *114*, 11004.
- (50) Kulshreshtha, C.; Kim, W., G.; Lampande, R.; Huh, H., D. ; Chae, M.; Kwon, H., J. *J. Mater. Chem. A* **2013**, *1*, 4077.
- (51) Zhao, Y.; Truhlar, D. *Theor. Chem. Account.* **2007**, *120*, 215.
- (52) Kwon, O. K.; Park, J. H.; Kim, D. W.; Park, S. K.; Park, S. Y. *Adv. Mater.* **2015**, *27*, 1951.
- (53) Shi, X.; Liu, S.; Liu, C.; Hu, Y.; Shi, S.; Fu, N.; Zhao, B.; Wang, Z.; Huang, W. *Chem. Asian J.* **2016**, *11*, 2188.
- (54) Lu, X.; Fan, S.; Wu, J.; Jia, X.; Wang, Z. S.; Zhou, G. *J. Org. Chem.* **2014**, *79*, 6480.
- (55) Frischmann, P. D.; Mahata, K.; Wurthner, F. *Chem. Soc. Rev.* **2013**, *42*, 1847.
- (56) Huss, A. S.; Pappenfus, T.; Bohnsack, J.; Burand, M.; Mann, K. R.; Blank, D. A. *J. Phys. Chem. A* **2009**, *113*, 10202.

- 1
2
3 (57) Li, C.; Liu, M.; Pschirer, N. G.; Baumgarten, M.; Mullen, K. *Chem. Rev.* **2010**, *110*,
4 6817.
5 (58) Experiments to measure singlet fission in asymmetric indenotetracenes are currently
6 underway.
7 (59) Zimmerman, P. M.; Bell, F.; Casanova, D.; Head-Gordon, M. *J. Am. Chem. Soc.* **2011**,
8 *133*, 19944.
9 (60) Congreve, D. N.; Lee, J.; Thompson, N. J.; Hontz, E.; Yost, S. R.; Reuswig, P. D.;
10 Bahlke, M. E.; Reineke, S.; Van Voorhis, T.; Baldo, M. A. *Science* **2013**, *340*, 334.
11 (61) Ehrler, B.; Walker, B. J.; Bohm, M. L.; Wilson, M. W.; Vaynzof, Y.; Friend, R. H.;
12 Greenham, N. C. *Nat. Comm.* **2012**, *3*, 1019.
13 (62) Table S15
14 (63) Ide, J.; Mereau, R.; Ducasse, L.; Castet, F.; Olivier, Y.; Martinelli, N.; Cornil, J.;
15 Beljonne, D. *J. Phys. Chem. B* **2011**, *115*, 5593.
16 (64) Vura-Weis, J.; Ratner, M. A.; Wasielewski, M. R. *Journal of the American Chemical*
17 *Society* **2010**, *132*, 1738.
18 (65) Adamo, C.; Barone, V. *J. Chem. Phys.* **1999**, *110*, 6158.
19 (66) ARBELOA, F. L.; OJEDA, R. P.; ARBELOA, L. I. *J. Lumin.* **1989**, *44*, 105—112.
20 (67) Grabolle, M.; Spieles, M.; Lesnyak, V.; Gaponik, N.; Eychmuller, A.; Resch-Genger, U.
21 *Anal. Chem.* **2009**, *81*, 6285.
22 (68) Perdew, J. P. B., K.; Ernzerhof, M. *Phys. Rev. Lett.* **1996**, *77*, 3865.
23 (69) Frisch, M. J.; Trucks, G. W.; Schlegel, H. B.; Scuseria, G. E.; Robb, M. A.; Cheeseman,
24 J. R.; Scalmani, G.; Barone, V.; Mennucci, B.; Petersson, G. A.; Nakatsuji, H.; Caricato, M.; Li, X.;
25 Hratchian, H. P.; Izmaylov, A. F.; Bloino, J.; Zheng, G.; Sonnenberg, J. L.; Hada, M.; Ehara, M. et al.
26 Gaussian 09; Gaussian, Inc.: Wallingford, CT, 2009.
27 (70) Valiev, M.; Bylaska, E. J.; Govind, N.; Kowalski, K.; Straatsma, T. P.; Van Dam, H. J. J.;
28 Wang, D.; Nieplocha, J.; Apra, E.; Windus, T. L.; de Jong, W. A. *Comput. Phys. Commun.* **2010**, *181*,
29 1477.
30
31
32
33
34
35
36
37
38
39
40
41
42
43
44
45
46
47
48
49
50
51
52
53
54
55
56
57
58
59
60